



Assessing the impact of bioturbation on sedimentary isotopic records through numerical models

Dominik Hülse^{a,*}, Pam Vervoort^a, Sebastiaan J. van de Velde^{b,c}, Yoshiki Kanzaki^{a,i}, Bernard Boudreau^d, Sandra Arndt^b, David J. Bottjer^e, Babette Hoogakker^f, Matthias Kuderer^g, Jack J. Middelburg^g, Nils Volkenborn^h, Sandra Kirtland Turner^a, Andy Ridgwell^a

^a Department of Earth and Planetary Sciences, University of California, Riverside, CA 92521, USA

^b Department of Geosciences, Environment and Society, Université Libre de Bruxelles, 1050 Brussels, Belgium

^c Operational Directorate Nature, Royal Belgian Institute of Natural Sciences, 1000 Brussels, Belgium

^d Department of Oceanography, Dalhousie University, Halifax, Nova Scotia B3H4R2, Canada

^e Department of Earth Sciences, University of Southern California, Los Angeles, CA 90089, USA

^f Lyell Centre, Heriot Watt University, Research Avenue South, Edinburgh EH14 4AP, UK

^g Department of Earth Sciences, Utrecht University, Utrecht, The Netherlands

^h School of Marine and Atmospheric Sciences, Stony Brook University, Stony Brook, NY 11794, USA

ⁱ School of Earth and Atmospheric Sciences, Georgia Institute of Technology, Atlanta, GA 30332, USA

ARTICLE INFO

Keywords:

Bioturbation
Sedimentary proxy record
Paleoceanography
Paleoclimatology

ABSTRACT

The disturbance of seafloor sediments by the activities of bottom-dwelling organisms, known as bioturbation, significantly alters the marine paleorecord by redistributing particles in the upper sediment layers. Consequently, ‘proxy’ signals recorded in these sediment particles, such as the size, abundance, or isotopic composition of plankton shells, are distorted by particle mixing. Accordingly, bioturbation can alter the apparent timing, duration, and magnitude of recorded events by smoothing climatic and oceanographic signals. In an extreme scenario, biological mixing can significantly obscure our view of the past by homogenizing the bioturbated layer, destroying sediment layering, and distorting the relative timing and intensity of past climatological events. Here we explore how bioturbation distorts proxy records of environmental events from a modeling perspective. First, we provide an overview and comparison of different numerical models created for simulating the movement and structural alteration of sediment by bioturbation. Next, we use an updated particle resolving model – iTURBO2 – to illustrate how various modes and intensities of bioturbation distort the signature of past climatological events, considering a range of conceptual shapes of vertical proxy profiles. Finally, we demonstrate how sampled proxy records can differ due to the combined effects of particle mixing and differential abundance changes that often concur with environmental transitions. We make the iTURBO2 MATLAB code openly available to facilitate further exploration of proxy biases due to bioturbation to aid the interpretation of the climatological record preserved in marine sediments.

1. Introduction

Our knowledge of past climates and their relationship to life on this planet primarily comes in the form of “proxies”, including those sampled from ice cores (e.g., Petit et al., 1999) and sediments (on land, in lakes and the ocean; Wefer et al., 1999; Henderson, 2002; Hillaire-Marcel et al., 2007; Eglinton and Eglinton, 2008), and ultimately accessed through geological outcrops and/or drill-cores (Soreghan and Cohen, 2013). In the marine realm, proxies can, for instance, be based on

indicative fossil species (Jorissen et al., 2007; Kucera, 2007), fossil shell size and weight (Broecker and Clark, 1999; Broecker and Clark, 2001), or the trace metal and isotopic composition of individual fossils or bulk sediments (Meyers, 1997; Siebert et al., 2003; Hönisch et al., 2019). They can be used to reconstruct an extraordinary variety of critical environmental indicators, including (but not limited to): the concentration of atmospheric carbon dioxide (CO₂; e.g., Royer et al., 2001), ocean acidity (pH; e.g., Foster and Rae, 2016) and carbonate chemistry (e.g., Rae et al., 2011), temperature (e.g., Elderfield and Ganssen, 2000),

* Corresponding author at: Max-Planck-Institute for Meteorology, Hamburg, Germany.
E-mail addresses: dominik.huelse@mpimet.mpg.de, dominik.huelse@gmx.de (D. Hülse).

<https://doi.org/10.1016/j.earscirev.2022.104213>

Received 14 April 2022; Received in revised form 7 September 2022; Accepted 7 October 2022

Available online 23 October 2022

0012-8252/© 2022 The Authors. Published by Elsevier B.V. This is an open access article under the CC BY license (<http://creativecommons.org/licenses/by/4.0/>).

oxygen saturation (e.g., Siebert et al., 2003; Lau et al., 2019) and levels (e.g., Moffitt et al., 2015; Hoogakker et al., 2015), the productivity and species composition of marine ecosystems (e.g., Lea and Boyle, 1990; Jorissen et al., 2007; Zonneveld et al., 2010), and the large-scale circulation of the ocean (e.g., Curry and Oppo, 2005). A tremendous effort has been put into the collection of sediment cores (e.g., from ocean drilling efforts such as the International Ocean Discovery Program) and down-core analysis of sedimentary proxies (e.g., the development of analytical instruments for single foraminiferal analysis; Reichart et al., 2003), all with the aim of reconstructing environmental changes spanning the most formative events and transitions in Earth history and at the highest resolution possible.

However, interpreting the past from proxy measurements is not trivial. The signals recorded in marine sediments, the primary focus of this review, reflect not only the environment in which the proxy-producing organisms lived but also what happens to the material during transport to the sediment and after deposition (e.g., Bao et al., 2019). Once buried, fossil remains of, for example, foraminifera and diatoms are directly affected by the sediment pore-water chemistry and can, in some cases, (partially) dissolve. In dissolution-prone environments, where bulk-sediment stable isotopes or trace elements are used to reconstruct environmental conditions, the results are likely to be distorted towards the more dissolution resistant species, thus painting a distorted picture of the past. Furthermore, the disturbance of the seafloor by the activities of living organisms, known as bioturbation (Richter, 1952), has profound effects on the physical and geochemical properties of the sediment (Rhoads, 1974; Aller et al., 1982).

Mechanisms for displacing sediment by bioturbators include development and maintenance of burrows and dwellings, ingestion and egestion of sediment particles, infilling of abandoned living structures, and lateral “ploughing” of the sediment surface (Levinton et al., 1995; Cadée and Reise, 2001). The displacement of sediment particles can be size-selective (Bard, 2001), highly discontinuous and stochastic (Meysman et al., 2008a,b; Reed et al., 2006, 2007), and co-vary with environmental change (e.g., Wetzel, 1984; Smith and Rabouille, 2002; Boudreau, 2004). The signs of bioturbation are called trace fossils when preserved in the geologic record (Crimes and Droser, 1992) and offer an important source for understanding the history of marine life. Studies integrating ichnological, sedimentological and taphonomical data to understand these trace fossils are common since the ichnofacies paradigm was proposed by Seilacher (1964) and review studies on these topics have been produced in the past (e.g., McIlroy, 2008; Bromley, 2012; Tarhan, 2018; Rodríguez-Tovar and Hernández-Molina, 2018; Rodríguez-Tovar, 2022).

Often overlooked is that this biogenic sediment mixing alters marine proxy records by smoothing and shifting the original climatic signals, thus obfuscating the timing, duration, and magnitude of recorded events (Fig. 1 and e.g., Berger and Heath, 1968; Shackleton et al., 1977; Hutson, 1980; Pisias, 1983; Schifflbein, 1984). Hence, since the colonization of the seafloor by benthic animals in the early Cambrian (Tarhan, 2018; Gougeon et al., 2018), reading the sediment record as a timeline has become complicated, particularly when the thickness of sediment accumulating over the duration of an environmental perturbation closely corresponds to the depth of biological mixing.

Because the deep-sea sedimentary record is sparse before 200 Ma due to the destructive effects of plate tectonics, the earlier evolution of marine bioturbation is largely known from shallower sediments deposited on continents. While it is not precisely known when animals first began inhabiting the seafloor, evidence for biologically mixed sediments becomes abundant around the terminal Proterozoic (Tarhan et al., 2015; Gougeon et al., 2018). Throughout the early Palaeozoic, bioturbation intensity and the mixed layer depth (defined as the depth to which the sediment is mixed thoroughly) gradually increased, with occasional major advances, such as the emergence of highly efficient sediment mixing (e.g., biological bulldozing), occurring in the Devonian-Carboniferous (Thayer, 1979; Thayer et al., 1983; Tarhan, 2018).

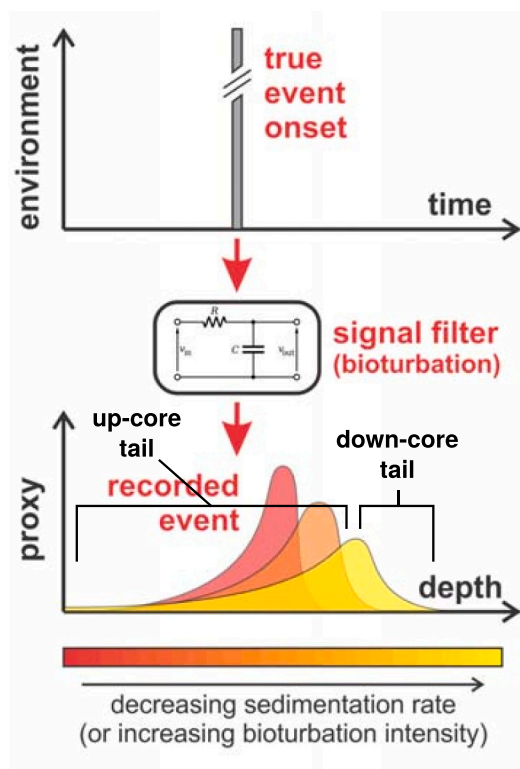


Fig. 1. Illustration of the distortion of a single environmental event as recorded in a sediment subject to diffusive bioturbation. The reduction in amplitude, shift in phase (time) and the depths of the tail is a function of sediment rate, and bioturbation. Therefore, a paleo-event can appear to have occurred thousands of years earlier, with a longer duration and lower magnitude than what would have been recorded without bioturbation.

However, various lines of evidence indicate that throughout the early Paleozoic, the average mixed layer depth remained far shallower than the mean modern value of ~ 10 cm (Boudreau, 1998; Solan et al., 2019; Tarhan et al., 2015; Teal et al., 2010a). Trace fossil observations from shallow marine environments suggest that highly efficient sediment mixers became more important during the Mesozoic, further increasing mixing depth and intensity (Ausich and Bottjer, 1982; Thayer et al., 1983; Bambach, 1993), with occasionally extreme burrow depths of up to 2.5 meters (Pemberton et al., 1976; Weaver and Schultheiss, 1983) or even 8 meters (Cobain et al., 2018). The umbrella term of bioturbation can be divided into two categories, based on the impact of benthic fauna on the sedimentary transport of particles and pore water: “particle reworking” (bio-mixing or bioturbation *sensu stricto*), and “burrow ventilation” (or bio-irrigation) (Meysman et al., 2006; Kristensen et al., 2012). While bio-irrigation and particle mixing are both of importance when considering early diagenesis and benthic-pelagic exchange fluxes of carbon, nutrient, iron and sulphur (e.g. Berner and Westrich, 1985; van de Velde and Meysman, 2016; van de Velde et al., 2018; Tarhan et al., 2021), particle mixing is more important for particulate tracers, like foraminifera or diatom shells. Therefore, this article is primarily focused on biological particle mixing, for which we use the term bioturbation *sensu stricto*.

Bottom water oxygen availability, organic matter supply, and sedimentation rate are the main constraints for the presence of benthic fauna (Rhoads, 1974; Savrda and Bottjer, 1991; Trauth et al., 1997; Boudreau, 1998). Consequently, most of the particles that are buried in marine sediments today and over a large part of the Phanerozoic have experienced bioturbation (Tarhan, 2018; Teal et al., 2010b). In oxygenated deep-sea environments with low sediment accumulation rates, even low bioturbation rates efficiently mix older sediment particles with newly

deposited particles. Hence, in these settings, sedimentary structures (i. e., laminations) will not be preserved, which is indicative of a thoroughly bioturbated mixed layer. The existence, intensity, and, more critically, the depth of the mixed layer are crucial factors, with significant implications for the interpretation of particulate tracers in the palaeo-record.

Bioturbation can act as a low-pass filter by reducing and shifting the signal amplitude and eliminating high-frequency variations. Consequently, this filtering is particularly problematic for reconstructing very rapid and short-lived (sub-) millennial scale climate events (Schiffelbein, 1984; Bard et al., 1987; Anderson, 2001; Trauth, 2013; Lougheed and Metcalfe, 2022). However, bioturbation more generally adds uncertainty in the creation of age models for deep-sea sediments. Age models are usually based on biostratigraphic datums, i.e., the origination or extinction of marker taxa, and/or paleomagnetic reversals. These boundaries are susceptible to displacement and smoothing by bioturbation, which may be one factor contributing to the common occurrence of overlapping or apparent stratigraphic reversals among datums. The age-depth datums used in constructing biomagnetostratigraphic age models (e.g., DSDP/ODP/IODP) often indicate different ages for sediment of the same depth or even reversals in the apparent age-depth relationship. In other words, a younger datum occurs stratigraphically below an older datum. Differential mixing among datums from different size classes (e.g., foraminifera versus nannofossils) or the differing likelihood of mixing up versus down-section may contribute to this source of age model uncertainty.

Higher-resolution relative dating of deep-sea sediments relies on cyclostratigraphy, or the recognition of astronomical cycles (precession, obliquity, and eccentricity) in various sediment properties, such as color, magnetic susceptibility, or elemental abundances. These cycles, ranging from ~21 to ~405 kyrs, typically correspond to just a few centimeters of sediment when considering typical deep-sea accumulation rates and hence are very susceptible to distortion by mixing (Pisias, 1983). For a sedimentation rate of less than 1 cm kyr⁻¹, precession cycles of ~21 kyrs will correspond to less than 20 cm of sediment, thus only twice the mean mixing depth in modern open ocean sediments (Boudreau, 1998; Solan et al., 2019). Bioturbation therefore causes significant distortions to the sedimentary record of individual astronomical cycles. This problem is exacerbated if cyclostratigraphic methods are used across an interval with decreased sedimentation rates, e.g., due to changes in either productivity or preservation of biogenic particles. Shorter duration, (sub-) millennial scale variability of smaller amplitude is even less likely to be detected in typical deep-sea settings for the same reason (Anderson, 2001). In addition, the imprint of more notable events, such as the extraterrestrial impact at the Cretaceous-Palaeogene (K-Pg) boundary (Hull et al., 2011; Alegret et al., 2015; Esmeray-Senlet et al., 2017) or the rapid and extreme global warming events identified from the Late Paleocene through Middle Eocene – known as “hyperthermals” (Thomas et al., 2000; Lourens et al., 2005; Kirtland Turner and Ridgwell, 2013), can be severely attenuated by bioturbation.

This article focuses on the numerical simulation and prediction of the distortions to proxy records of environmental events created by bioturbation and illustrates some primary phenomena relevant to deep-sea sedimentary records. We note that to fully understand the causes and impacts of bioturbation on the sedimentary record, a more integrative approach would be needed that also considers factors such as ichnological, sedimentological, and taphonomical analysis, which this article does not cover. We refer the interested reader to McIlroy (2008); Tarhan (2018), Rodríguez-Tovar and Hernández-Molina (2018); Rodríguez-Tovar (2022) for reviews on these topics. In this paper, we first provide an overview and comparison of different numerical models devised to assess sediment displacement by bioturbation. Next, we use an updated explicit particle model – *i*TURBO2 – to illustrate how bioturbation can distort the expression of various idealized environmental events. We

show how different modes and intensities of bioturbation lead to varying degrees of distortion and explore how under-sampling in combination with bioturbation introduces additional uncertainty to the recorded isotope signal. Subsequently, we use *i*TURBO2 to investigate the effects of sediment mixing on a synthetic isotopic signal derived from the Laskar et al. (2004) astronomical solution. Finally, we apply the model to ash layers deposited in the Indian Ocean and to explain single-foraminifera isotope data across the Paleocene–Eocene thermal maximum (PETM).

2. Numerical models of bioturbation

For highly idealized sediment mixing, signals may be deconvolved analytically (e.g., Berger and Heath, 1968; Guinasso and Schink, 1975; Berger et al., 1977; Goreau, 1980; Schiffelbein, 1985; Bard et al., 1987; Liu et al., 2021). Here, continuum analytical approaches (Section 2.1) are useful for evaluating bulk sediment properties, such as bulk isotopes and elemental geochemistry. However, complications arise because particle translocation may be highly selective in terms of particle characteristics, such as size, shape, or chemical composition (Wheatcroft, 1992; Thomson et al., 1995; Brown et al., 2001; Bard, 2001). The nature of individual disturbances also depends on animal species and behavior, in turn, influenced by the environment, particularly food supply, oxygen availability, and the geo-mechanical properties of the sediment (Savrda and Botzler, 1991; Trauth et al., 1997; Biles et al., 2002; Dorgan et al., 2005; Dorgan et al., 2006). The overall effect of sediment mixing on a proxy record is, thus, a function of many variables and is difficult to disentangle.

Numerical models are ideal tools to improve our understanding of this complex, interrelated system and can be used to simulate the effects of biological mixing on the sedimentary record. Because there are essentially two different perspectives to study bioturbation: the macroscopic perspective of the bulk sediment movement and the microscopic perspective of individual particles (Meysman et al., 2003; Meysman et al., 2010; Maire et al., 2008), there are consequently, two difference classes of numerical representation, termed continuum models and explicit particle models, respectively. The nature of the scientific question dictates the complexity of the numerical model to use. For example, the continuum model's simplicity, which permits explicit deconvolution (e.g., Berger and Heath, 1968; Berger et al., 1977; Goreau, 1980; Bard et al., 1987; Liu et al., 2021), may be appropriate for understanding bulk geochemical records. While an explicit particle model is needed if the question requires the evaluation of individual particles or certain fractions of the sediment. However, it appears that the analytical continuum model approach is flexible enough to generate bioturbation profiles similar to profiles generated with an explicit particle model (cf. Liu et al., 2021 with profiles in Section 4.1.1). We review both numerical model classes in the following sub-sections.

2.1. Continuum models of bioturbation

For geochemical analysis requiring relatively large samples and/or sampled from geological outcrops, the appropriate level of representation is generally not the individual particle but the macroscopic level (Maire et al., 2008; Meysman et al., 2008a). Due to the random and variable character of bioturbation, it is typically represented as a one-dimensional diffusive process in continuum models (e.g., Goldberg and Koide, 1962; Guinasso and Schink, 1975; Boudreau, 1986; Hülse et al., 2018). As such, bioturbation is numerically represented by a biodiffusion coefficient (D_b) e.g., in cm²yr⁻¹, which characterizes the mixing intensity and a depth over which diffusive mixing occurs (z_{bio} in cm, Guinasso and Schink, 1975). It has been shown that this approach can simulate the exponential decrease in radioisotope tracer profiles often observed in bioturbated sediments (e.g. Cochran, 1985; Green et al., 2002). Furthermore, the biodiffusion model has the advantage of mathematical simplicity and computational efficiency, and therefore,

has become the most common numerical approach.

The biodiffusion model implicitly encapsulates the plethora of animal activities affecting the sediment (e.g., feeding, burrowing, burrow excavation and collapse) by a single biodiffusion coefficient. Furthermore, theoretical analysis has shown that in applying the biodiffusion model, a number of assumptions regarding the frequency, length scale, and symmetry of mixing events are made (Boudreau, 1986; Boudreau and Imboden, 1987; Meysman et al., 2003; Meysman et al., 2010), but rarely explicitly stated or even recognized. Many typical modes of bioturbation, in fact, violate these assumptions. For instance, observations show that many infaunal organisms do not randomly move sediment particles over short distances, as required by the biodiffusion model, but move particles advectively over relatively large distances, e.g., the conveyor-belt transport by deposit feeders (Robbins et al., 1979; Aller et al., 1982; Smith et al., 1986). Subsequent efforts have addressed this lack of biological realism with the development of so-called nonlocal continuum models, which allow for particle displacements between spatially separated layers in the sediment domain (Boudreau and Imboden, 1987). Stochastic modeling approaches to bioturbation have also been explored, but mainly from a theoretical perspective (e.g., Meysman et al., 2003, 2008a; Wheatcroft et al., 1990). These studies revealed that after many mixing events, the impact of bioturbation eventually appears diffusive (Meysman et al., 2010) and can be quantified with biodiffusion coefficients (D_b) that can be decomposed into the square of particle displacement distance divided by the waiting time between discrete mixing events (Meysman et al., 2008a; Wheatcroft et al., 1990).

2.2. Explicit particle models of bioturbation

While the continuum models described above are valuable tools for studying bulk sediment behavior, actual sediment structures and individual particles are not represented. For climate signals recorded in single sediment particles or small groups of sediment particles, an explicit particle model is needed in order to study the impacts of bioturbation. Various attempts exist to create representations that allow for the discrete, stochastic nature of biogenic sediment mixing and its effects on individual particles (Fig. 2).

Most explicit particle models represent the sediment column as a 1-D or 2-D lattice of discrete cells (Fig. 3), e.g., Shull, 2001; Choi et al., 2002; Schiffers et al., 2011; Trauth, 2013. The 1-D stochastic mixing models of Meile and Van Cappellen (2005) and Hull et al. (2011) are notable exceptions, representing the sediment as a spatially continuous domain. Explicit particle models can be further subdivided into bio-implicit and bio-explicit models (Fig. 2). In bio-implicit models, cells can be occupied by sediment particles with prescribed properties (e.g., sediment type, tracer concentration, porosity).

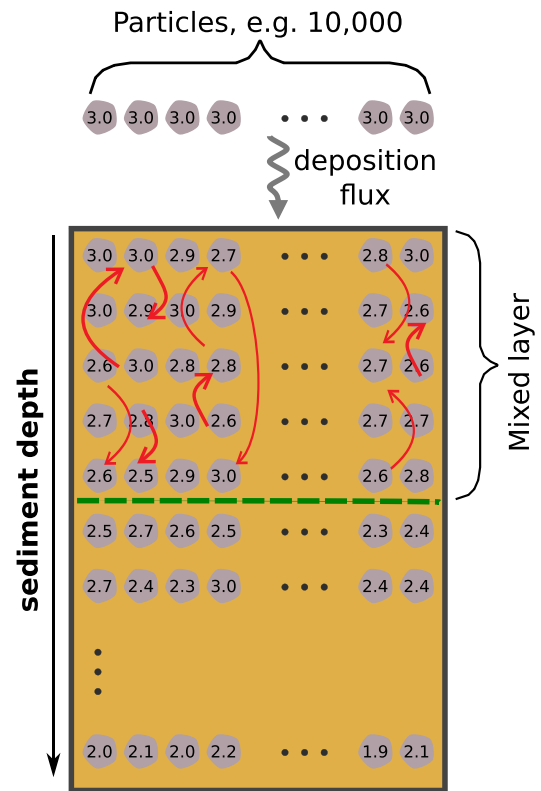


Fig. 3. Schematic of the 2-D lattice of the (i) TURBO2 model that simulates the influence of bioturbation depth on the isotopic signal of one signal carrier. Here, in each sediment layer, 10,000 particles are simulated. The red arrows indicate random mixing after every sedimentation event of a new layer of 10,000 particles.

Particle rearrangement due to bioturbation has been simulated according to probabilities in a transition matrix (e.g., Foster, 1985; Trauth, 1998; Shull, 2001; Kanzaki et al., 2021). The probabilities describe the fraction of particles that are moved and the location where each particle is moved to - both are generally random but can also be probability-based or weighted. For example, the ‘TURBO2’ model of Trauth (2013) simulates the effect of bioturbators that instantaneously homogenize the entirety of the mixed layer. As we illustrate later, the consequence of this assumption is that deeper but less frequent mixing events are not simulated, and the observed down-core tail of mixing apparent in numerous proxy records is not reproduced (Fig. 1).

Some bio-implicit particle models are further able to represent some

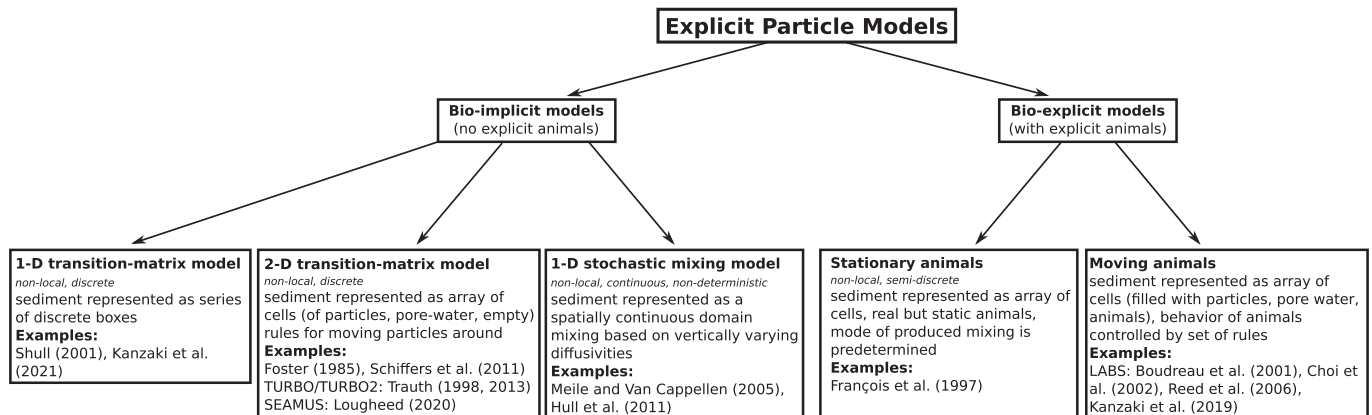


Fig. 2. Schematic relating different explicit particle mixing models.

of the (bio-) geochemical complexity in sediments. For instance, Shull (2001) includes the probability of a tracer undergoing radioactive decay, while the more recent model SEAMUS (Lougheed, 2020) assigns individual ^{14}C activities to the explicitly represented sediment particles, thus allowing simulation of synthetic sediment-archive histories. The “Implicit model of Multiple Particles (and diagenesis)” – IMP – (Kanzaki et al., 2021) is a reactive-transport model of carbonate and organic matter diagenesis that is able to represent various types of solid-phase mixing through the use of different transition matrices. However, although particle mixing with bio-implicit models is non-predictable and can be both local and non-local (see Meysman et al., 2003; Meysman et al., 2010), infaunal organisms are still absent, and the transition probabilities are random or predefined by the user, rather than dynamic features of the model or related to the organisms involved.

Bio-explicit particle models address this lack of biology. The functional-group model of François et al. (1997) simulates the sediment reworking mode of four typical bioturbators: the biodiffusers, the upward-conveyors, the downward-conveyors, and the regenerators, which establish burrows by transferring particles from depth to the surface, and voids are subsequently refilled with surface or neighboring particles (Gardner et al., 1987). While infaunal organisms are represented in the model, they are static, and the type of mixing they produce is predetermined.

In contrast, Choi et al. (2002) and Reed et al. (2006); Reed et al., 2007 developed the Lattice-Automaton Bioturbation Simulator (LABS) that explicitly incorporates organisms as entities in the sediment model. LABS represents the sediment as a 2D-lattice of cells filled with either porewater, sediment particles or an organism, or part thereof. The organisms move through the virtual sediment column by displacing or ingesting/defecating particles, governed by a set of deterministic and stochastic rules. Each sediment particle in LABS can have chemical, biological, and physical properties (e.g., food versus inert material), which also influences the movement of the organisms. Recently, the LABS model has been extended with deterministic calculations of water flow, dissolved oxygen and organic matter concentration fields to better reflect the physicochemical evolution of the sediment as a function of bioturbation – iLABS (Kanzaki et al., 2019). Thus, it represents a numerical model that simulates the coupled evolution of burrow geometry and physicochemical conditions in the sediments. Because iLABS can simulate and visualize burrow geometries assuming different sedimentological conditions, model results may be used to better understand trace fossils in the geological record. As iLABS explicitly represents bioturbators, including their deaths, taphonomical aspects may be addressed as well, even though additional model developments might be necessary (see Section 5). iLABS arguably constitutes the most comprehensive encapsulation of bioturbational mixing to date. However, due to its high computational demand, iLABS has not yet been applied in a geologic context, reflecting the generic practical problem in numerical models of biogeochemical processes and cycles, i.e., the finer the spatial resolution and more comprehensive and mechanistic the included processes, the greater the computational demand and difficulty in simulating processes on geological time-scales, relevant to address fundamental paleoclimate questions.

3. Illustrating primary distortions caused by bioturbation – Experiments with the iTURBO2 model

For the remainder of the paper we will be presenting a series of bioturbation model experiments to illustrate some of the primary distortions that a proxy record can experience. For this purpose we updated the bio-implicit particle model ‘TURBO2’ of Trauth (2013), now calling it iTURBO2. In this first section, we describe this model, starting with a summary of TURBO2, before describing the changes made to create iTURBO2, and then finish with a description of the experimental setup of the model experiments.

3.1. The original TURBO2 model

In its original version, TURBO2 simulates instantaneous, homogeneous mixing by using random mixing matrices. In other words, each explicitly represented sediment particle randomly changes its position within the mixed layer every time a new sediment layer is deposited at the sediment–water interface. TURBO2 simulates sedimentation and mixing of individual stratigraphic signal carriers, e.g., foraminifera, containing an isotope signature (compare Fig. 3). As such, the model can be used to study the impact of bioturbation on isotope signals (e.g., ^{14}C , $\delta^{18}\text{O}$, or $\delta^{13}\text{C}$) measured, for instance, in foraminifera shells (Trauth, 2013). Furthermore, TURBO2 can help the user recognize distortions in an isotope record caused by small sample sizes used for isotope measurements, i.e., often fewer than 15 individual specimens per sample are used.

To run TURBO2, the user must provide a data array containing information on the specific experiment. The rows of this input data array correspond to newly deposited sediment layers of 1 cm thickness. For each new sediment layer, the user must specify the mixed layer depth in centimeters (the second column), the abundance of a signal carrier (the third column), and its isotope signal (the fourth column). Thus, before mixing, all particles in a newly deposited sediment layer have the same isotopic signal (Fig. 3). TURBO2 imposes a signal as a function of depth; however, the sediment column can be transformed to the time domain if the ages of the sediment layers are specified (the first column). In addition, the number of signal carriers being picked and measured throughout the sediment core needs to be defined.

3.2. The updated iTURBO2 model

First, we (re-) introduced an approach to simulate user-specified types of mixing, e.g., local mixing or depth-dependent variations in mixing intensities, using transition matrices that are provided by the user, as per Trauth (1998). To illustrate the effects of contrasting types of mixing, we created three transition matrices, with mixed layer depths of 5, 10, and 20 cm, representing local mixing with a slightly higher probability for sediment particles to be moved upwards. This is in addition to being able to apply simple fully mixed (homogeneous) layer assumptions.


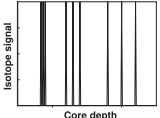
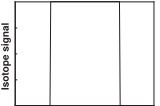
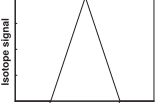
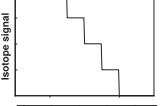
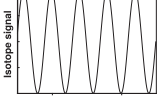
Second, we embedded the original code in an additional script that allows one to repeatedly execute the same experiment but using different, randomly generated mixing matrices. The rationale behind this was to generate a range of random mixing outcomes, which should encompass the real world result. Each single model realization and the mean model prediction are plotted and can be compared visually, which allows for a simple, qualitative, uncertainty analysis.

iTURBO2 is written in MATLAB and is made openly available as described in the ‘Code availability’ section at the end of the paper. As part of the code release, we provide the parameter files and transition matrices necessary to reproduce all the experiments conducted in the paper. We also include a brief installation and user-guide and have extended iTURBO2 to read input data from Excel files to help facilitate the modification of existing and the creation of new input data.

3.3. iTURBO2 experiments

For illustration, we created a set of six idealized paleoceanographic ‘shapes’, where the isotope signal of all stratigraphic carriers, such as from a specific foraminifera species, is changed down-core (Table 1). The black lines in Fig. 4 are the original change in the isotope signal, i.e., without bioturbational mixing. The shapes correspond generically to some of the types of signals studied in paleoceanographic records, ranging from isolated events over transitions to cyclical changes. For instance, the classic way to study and estimate bioturbation rates is from the distribution of conservative particles, such as volcanic ash or

Table 1
Idealized paleoceanographic shapes with top-down isotopic signal changes.

Name	Description of isotope change	Figure
Point event	Instantaneous, impulse change only at 1 point	
Multiple point events	Same amplitude, different spacing	
Step change	Instantaneous, abrupt but sustained change	
Ramp up/down	Gradual change (max not sustained)	
Multiple step changes	Multiple equal step changes	
Sinusoidal change	Change with constant wavelength	

microtektites (Glass, 1969; Ruddiman and Glover, 1972; Guinasso and Schink, 1975; Ruddiman et al., 1980) that represent the instantaneous deposition of a tracer in a single event. The deposition of ejecta resulting from an extraterrestrial impact, such as at the K-Pg boundary, is another ‘real world’ example of this tracer experiment (Guinasso and Schink, 1975; Hull et al., 2011; Esmeray-Senlet et al., 2017). These events are valuable because they correspond to a forcing with a known duration (effectively, instantaneous), and the relationship between forcing and observed tracer is straightforward. In contrast, while the forcing behind orbital cycles is known, the connection between the forcing and the tracer is less certain. For other shapes we consider, such as step or ramp changes, both the forcing and the relationship with the observed tracer are unknown. Still, we can relate some of these conceptual shapes to realistic paleo-events. For example, the step sequence could correspond to a record of a glacial termination (e.g., Steffensen et al., 2008), while the ramp-up/down is similar to reconstructed early Cenozoic hyperthermals (Kirtland Turner and Ridgwell, 2013). In general, the more complex and time-dependent the likely forcing(s) and feedbacks associated with a geological event or transition are, the more difficult it is to assess what the unmixed record ‘should’ look like.

Each of our iTURBO2 experiments comprises a set of 100 simulations, applying different sets of randomized mixing matrices. We plot the result of each individual simulation as well as the mean model prediction.

4. Results and discussion

We now present and discuss a series of simulations made using iTURBO2 to illustrate some of the complexities imparted to the marine geological record by bioturbation.

4.1. Isotopic change only

First, we evaluate the effect of homogeneous and local (preferentially upward) mixing on a single signal carrier, e.g., one foraminifera species. We simulate three different mixed layer depths (i.e., 5, 10, and 20 cm)

for both mixing types. We only change the imposed isotopic signal throughout the sediment column for each of our six conceptual shapes and keep the abundance of the carrier constant. As such, we ignore preservation/dissolution changes and assume that the population of the foraminifera species does not change over time.

4.1.1. Idealized mixing of conceptual shapes

We simulate 10,000 particles (e.g., foraminifera shells) in each sediment layer and compare 5, 10, and 20 cm mixed layer depths for homogeneous and local mixing (Fig. 4). After mixing, in each sediment layer, the isotopic values of all particles are recorded. This idealized scenario of sampling all particles ensures that the recorded isotopic signal represents the average signal without uncertainties related to sampling and is, hence, analogous to measuring the bulk isotopic composition of a sediment layer.

As expected, the impact of bioturbation on the recorded signal of an impulse or point event (where the isotopic signal only changes in a single sediment layer, Fig. 4a + b) demonstrates the dispersion of the isotopic signal over an extended depth interval. Due to random particle mixing by bioturbation, which dilutes the point event with background isotopic values, the observed maximum isotopic change is less than 25% of the original change, and it inversely scales with the mixed layer depth. Under the homogenous mixing scenarios, the largest isotopic changes are observed at the base of the mixed layer, i.e., 5, 10, or 20 cm below the original location of the point event. Above this peak, the isotopic signal recovers exponentially to the background value. Conversely, in the local mixing scenario, the largest isotopic excursion is observed above the original position of the impulse, and the signal displays a more Gaussian-like distribution (Fig. 4b).

An important impact of bioturbational smearing is demonstrated when simulating multiple point events of the same magnitude as in Fig. 4c + d. In those simulations, the observed isotopic signal does not recover to background values between each event if the individual isotope changes occur in rapid succession and/or the mixed layer is sufficiently deep. Consequently, individual pulses become indistinguishable. In addition, the amplitude of the recorded isotopic event accumulates as more of the “signal” is transmitted up-section, such that later isotopic changes are seemingly more pronounced, even though the original amplitude is the same for each event.

The impact of random bioturbational mixing on an abrupt and sustained step change of the isotopic signal is shown in Fig. 4e + f. In the homogenous mixing scenarios, the isotopic change in the bioturbated record is observed earlier than in the original, abrupt shift. For both the homogeneous and local mixing scenarios, the minimum isotopic value in the bioturbated record is approached further up-core from the original shift. The down-core and up-core smearings are more pronounced for a deeper mixed layer. The overall effect is to increase the relative duration of both the onset and recovery and to decrease the relative duration of the peak sustained isotopic change. Similar but moderated, smearing effects are observed in the gradual ramp up/down experiment (Fig. 4g + h). As the original maximum isotopic excursion is not sustained, the bioturbated isotopic change reduces in magnitude. However, it is much larger than the comparable maximum bioturbated isotopic change for the point event experiment because mixing occurs between adjacent particles that have isotope values closer to the maximum change (Fig. 4a). When simulating an isotopic change in multiple, equal steps, the individual steps become more indistinct due to the smearing effect of deeper bioturbational mixing (Fig. 4i + j). For the sinusoidal isotopic change, deeper bioturbation results in a lower amplitude and a larger phase shift of the observed isotopic signal (Fig. 4k + l). Homogenous mixing causes a lead, while the up-core local mixing causes a lag phase shift.

To analyze the effects of bioturbation on orbitally mediated climate signals in more detail, we created an artificial sine-wave with three distinct, equally-weighted periods of 20, 40, and 100 kyrs, i.e., frequencies of 0.05, 0.025, and 0.01 cycles kyr⁻¹, comparable to the pe-

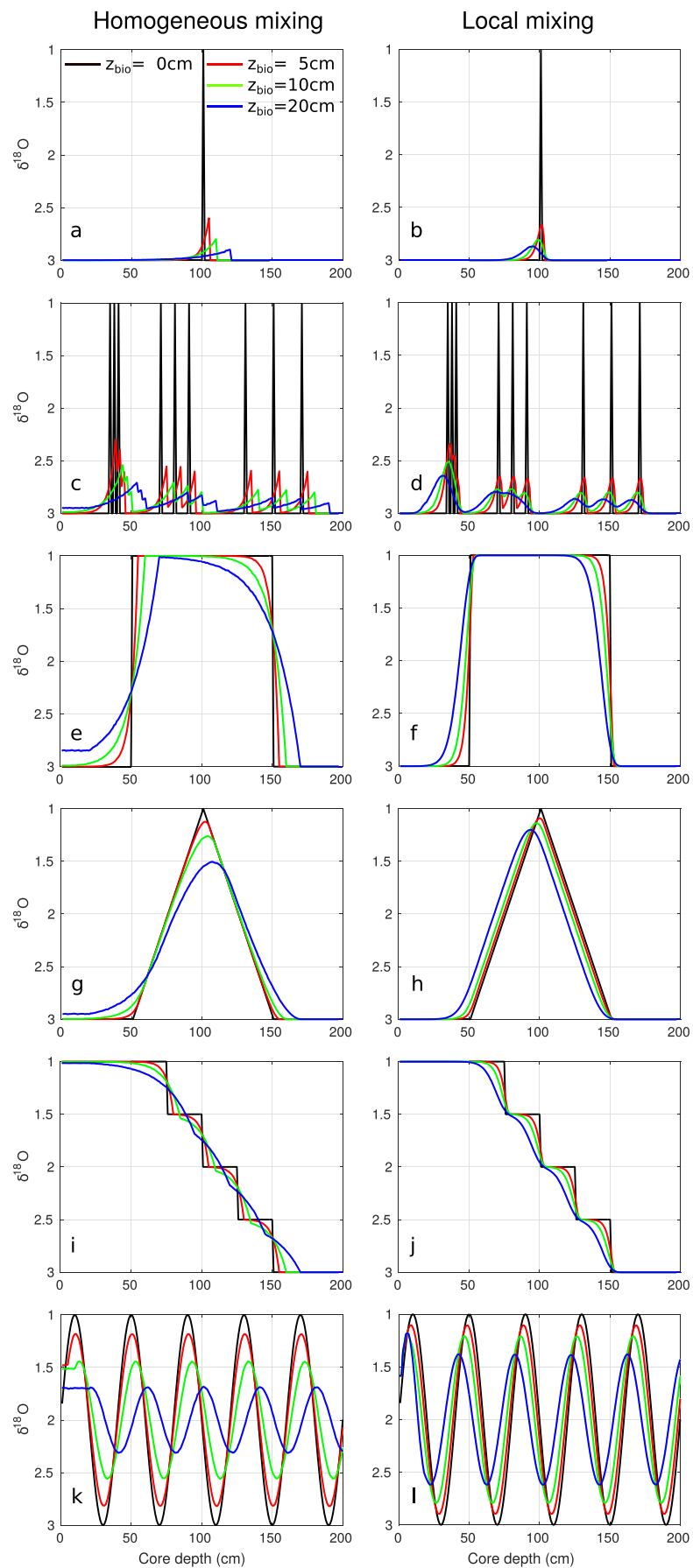


Fig. 4. Alteration of proxy distributions of six idealized paleoceanographic events (Table 1) by bioturbation for three different mixed layer depths.

riods of precession, obliquity, and short eccentricity cycles, respectively. We transformed the resulting sine-wave into the hypothetical $\delta^{18}\text{O}$ signal shown in Fig. 5a (black) and simulated the effect of homogeneous mixing using three different mixed layer depths. Our results clearly show the low-pass filter effect of bioturbation when we plot the isotopic signal's power spectrum, i.e., the distribution of power of its frequency components (Fig. 5). While bioturbation reduces the power (Fig. 5b–e) and causes a phase-shift (Fig. 5f–i) for all three frequencies, the effects are more pronounced for the higher-frequency oscillations. Local mixing leads to comparable results while causing a negative phase shift (not shown).

4.1.2. 'Real world' examples

Ash layers

The impact of bioturbational mixing can be analyzed by tracing the vertical dispersion of conservative particles, such as volcanic ash and microtektites that have been deposited in a single instantaneous event (e.g., Glass, 1969; Ruddiman and Glover, 1972; Guinasso and Schink, 1975; Ruddiman et al., 1980). In order to illustrate to what degree the simple mixing by iTURBO2 can (or cannot) simulate the simplest possible real-world sediment features, we compare simulated profiles to observed ash profiles from two marine depositional environments in the Indian Ocean (Fig. 6, Ruddiman et al., 1980). Sediments in the first environment were deposited at a mean rate of 0.5 cm kyr^{-1} , while the second setting has a mean rate of $2.0 - 2.5\text{ cm kyr}^{-1}$. These are both within the range of typical sedimentation rates in the deep sea (Ruddiman et al., 1980). As in the previous section, we simulate 10,000 sediment particles in every sediment layer and repeat the mixing simulations 100 times. The colored lines in Fig. 6 indicate the normalized average

ash concentration of the 100 individual simulations.

Homogenous mixing in iTURBO2 shifts the peak in ash concentration down-core from the depth of its original deposition (Fig. 6a, b), while our local mixing schemes shift the peak up-core (Fig. 6c, d). In addition, the recorded magnitude of the ash pulse is reduced. Both effects are enhanced with an increase in mixed layer depth. When compared to observations, ash profiles from the location with a low sedimentation rate are better simulated by deeper mixed layers, as expected (Fig. 6a, c), while reproducing ash profiles from higher sedimentation rate cores requires shallower mixed layers (Fig. 6b, d). This is consistent with the idea that bioturbators have more time in the low sediment accumulation environment to vertically disperse the deposited ash layer because sediment spends proportionally more time near the sediment–water interface before ‘escaping’ the bioturbated layer for long-term burial. The exponential decrease in simulated ash concentrations above the event peak for both mixing types closely follows observations from both depositional environments. However, the simple instantaneous, homogenous mixing approach fails to simulate the down-core smearing apparent in the ash records (Fig. 6a, b). Local mixing performs better and reproduces most smearing effects, especially for the low sedimentation environment (Fig. 6c). The data-model mismatch for the high sedimentation environment (Fig. 6b, d) might have resulted from rare, deep mixing events (i.e., non-local mixing), which are not represented in iTURBO2.

Orbital signals

Next, we investigate the effect of sediment mixing on a synthetic, high-resolution, climatic input signal, using the last 4 million years of the Laskar et al. (2004) astronomical solution as a template. Here, eccentricity, obliquity, and precession are equally weighted to facilitate

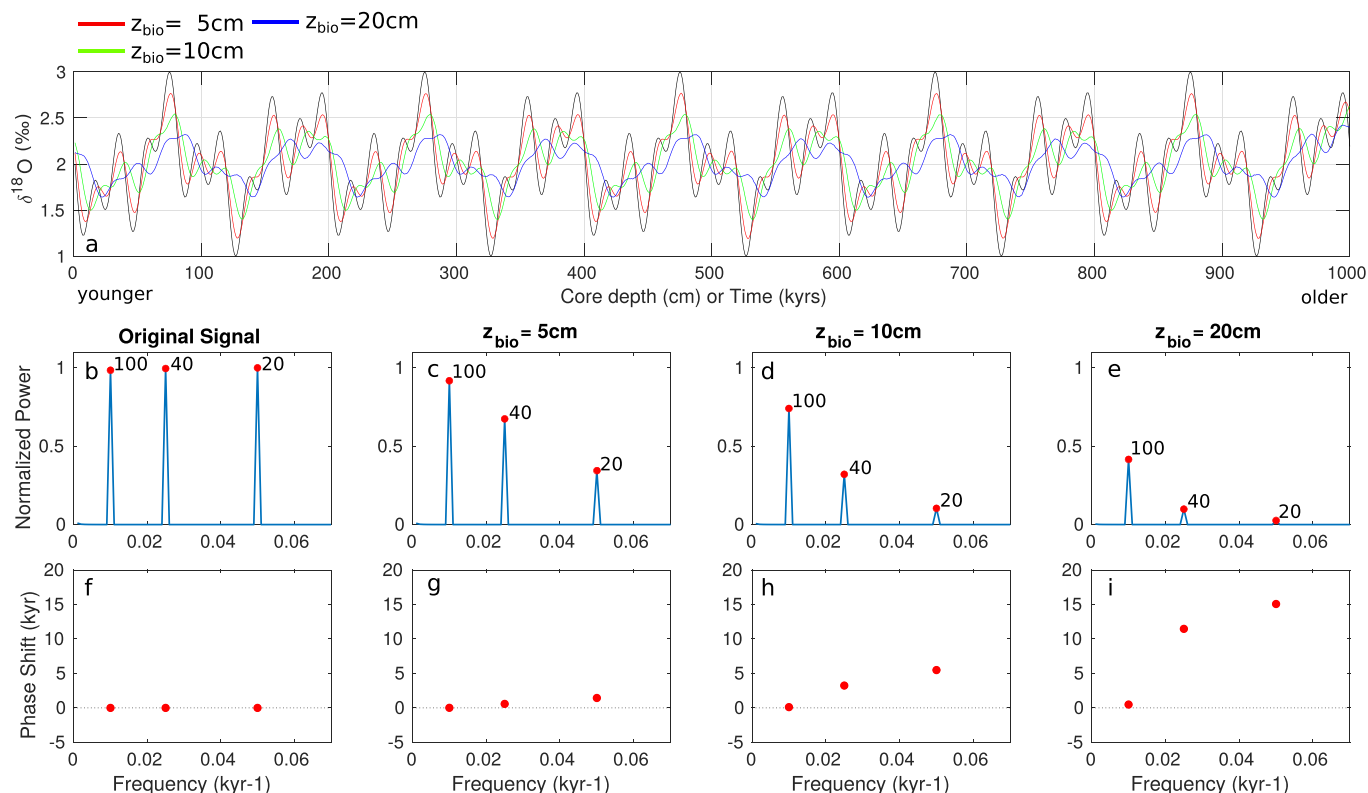


Fig. 5. Homogeneous mixing of an artificial, sinusoidal, isotopic change created with three periods (20, 40 and 100 kyrs). a: Time-series of original (black) and bioturbated signals using three different mixed layer depths. b–e: Power spectra of the four signals, normalized to the maximum power of the original signal. f–i: Phase shift of the three periods relative to the original signal, where positive values represent a corresponding lead of the bioturbated signal. It is possible to translate sediment core depth into the time domain by assuming a sedimentation rate of 1 cm kyr^{-1} . Note, however, that time here denotes model-time or ‘layer’ age, as the mean age of all particles in a specific layer can be very different due to bioturbation (Guinasso and Schink, 1975). Power spectra are estimated using periodograms, via Fast Fourier Transform of the modeled time series (Cooley and Tukey, 1965).

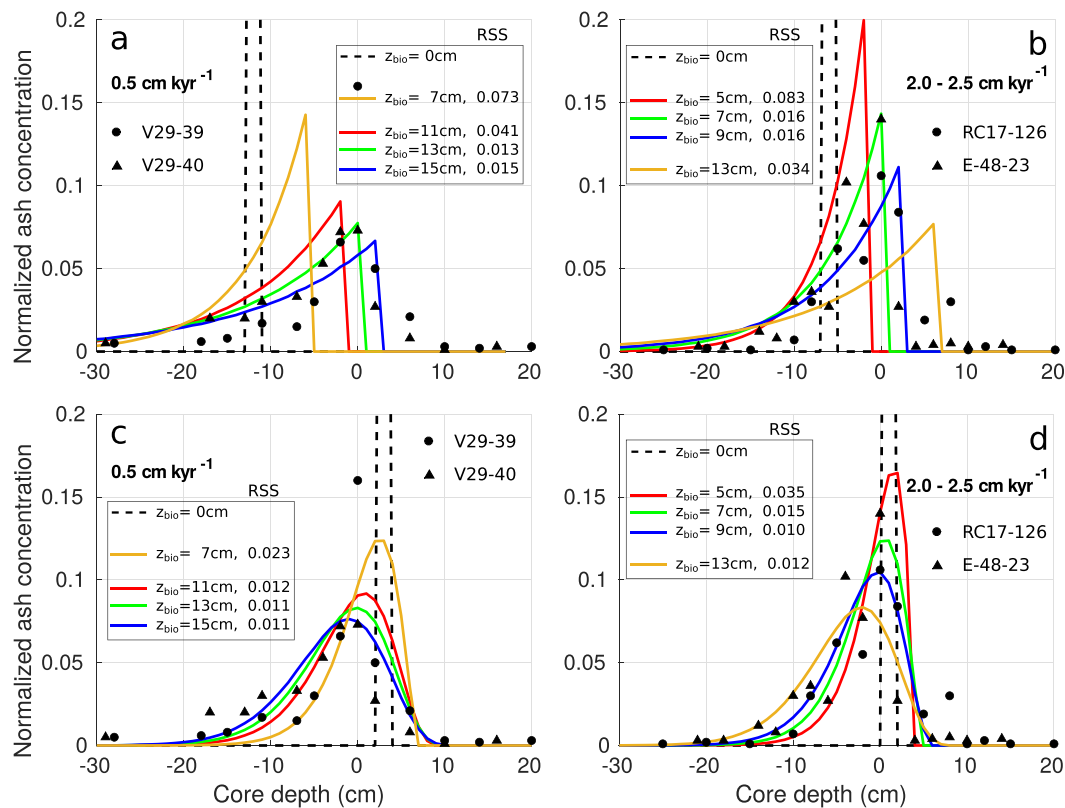


Fig. 6. Observed and simulated bioturbational mixing of an impulse event. Observed ash profiles (dots and triangles; Ruddiman et al., 1980) from two Indian Ocean sediment cores with a sedimentation rate of (a, c) 0.5 cm kyr^{-1} and (b, d) $2.0 - 2.5 \text{ cm kyr}^{-1}$, compared to simulated profiles of an impulse of ash at the sediment surface. Shown are simulated, normalized down-core ash concentrations in the absence of bioturbation (dashed black line) and four mixed layer depth scenarios (solid colored lines) using homogeneous (a, b) and local mixing (c, d). The decimals in the legends represent the residual sum of squares (RSS) between the data and each bioturbation scenario. Maximum tracer concentrations of the observations and the green mixing scenarios are aligned in depth (defined as 0 cm).

spectral detection of each orbital parameter in the original signal. The resulting signal is transformed into a synthetic $\delta^{18}\text{O}$ signal, with values ranging from 1.0‰ to 3.0‰ (Fig. 7a, black line, i.e., the same amplitude and range as in the earlier, idealized experiments). This $\delta^{18}\text{O}$ signal is used as input for iTURBO2.

The results in Fig. 7 show similar effects to those discussed for the artificial isotope signal (Fig. 5). The low-pass filter effect causes a significant loss of spectral power of the short precession cycles (23.7 and 22.3 kyrs). While the absolute power of longer periods, i.e., the 125 kyrs and 95 kyrs eccentricity cycles, also weakens, their relative power (compared to the precession cycles) increases (Fig. 7b–e). The phase shift of the bioturbated signal relative to the original signal is most pronounced for the high-frequency cycles. The power and phase of the longest eccentricity signal, i.e., 400 kyrs, is hardly affected by bioturbation.

4.2. The importance of abundance changes (Preservation effects)

In addition to changing proxy values, e.g., isotopic ratios, changes in proxy carrier quantity (e.g., foraminifera test abundance) are frequently observed over short vertical distances within sediments (e.g., Field et al., 2006; Lougheed and Metcalfe, 2022). This (sub-) millennial scale variability is primarily related to changes in mean annual sea-surface temperature (Morey et al., 2005) and has been shown to respond to rapid climate fluctuations, such as Dansgaard–Oeschger events (Hendy and Kennett, 2000) and El Niño–Southern Oscillation (ENSO, Roche et al., 2018; Metcalfe et al., 2020). In addition, selective dissolution in sediments can alter species composition and partially obscure this primary signal, thus complicating paleoenvironmental interpretations (Berger, 1968; Coulbourn et al., 1980). Here we explore how fluctuations in

species composition in sediments influence the recorded isotopic signal by varying the abundance of foraminifera particles with depth in the simulated sediment column.

4.2.1. Idealized mixing of conceptual shapes

Fig. 8 illustrates changes in the recorded abundance (left panel) and isotopic signal (right panel) for three conceptual shapes. The three idealized scenarios start with 1,000 foraminifera particles at a core depth of 200 cm (left panel). We simulate four different abundance-change scenarios in the sediment core, i.e., we decrease the original abundance by 0%, 50%, 90%, and 100% (left panel Fig. 8). For simplicity, the isotopic signal changes from 3.00‰ to a minimum value of 1.00‰ simultaneously with the foraminifera abundance in all experiments (right panel Fig. 8). We also simulated an offset between abundance and isotopic changes, which leads to comparable results (not shown). After homogeneous mixing, all 1,000 foraminifera particles are picked in each layer, and their isotopic values are recorded. The bioturbation depth is fixed to 10 cm.

Bioturbation has a more significant effect on the recorded isotopic signal when isotopic variations occur in combination with changes in foraminifera abundance. For instance, the amplitudes in the point event and the ramp-up/down cases are reduced compared to the input signal and scale with the decrease in abundance (Fig. 8b + f). For the step-change signal, the onset duration appears longer if the abundance is decreased synchronously with the isotopic change (Fig. 8d, around 150 cm). In contrast, the observed isotopic change is more rapid if the abundance recovers synchronously with the isotopic signal (Fig. 8d, around 50 cm).

Variations in foraminifera abundance are often directly related to environmental changes, such as transitions between cold and warm

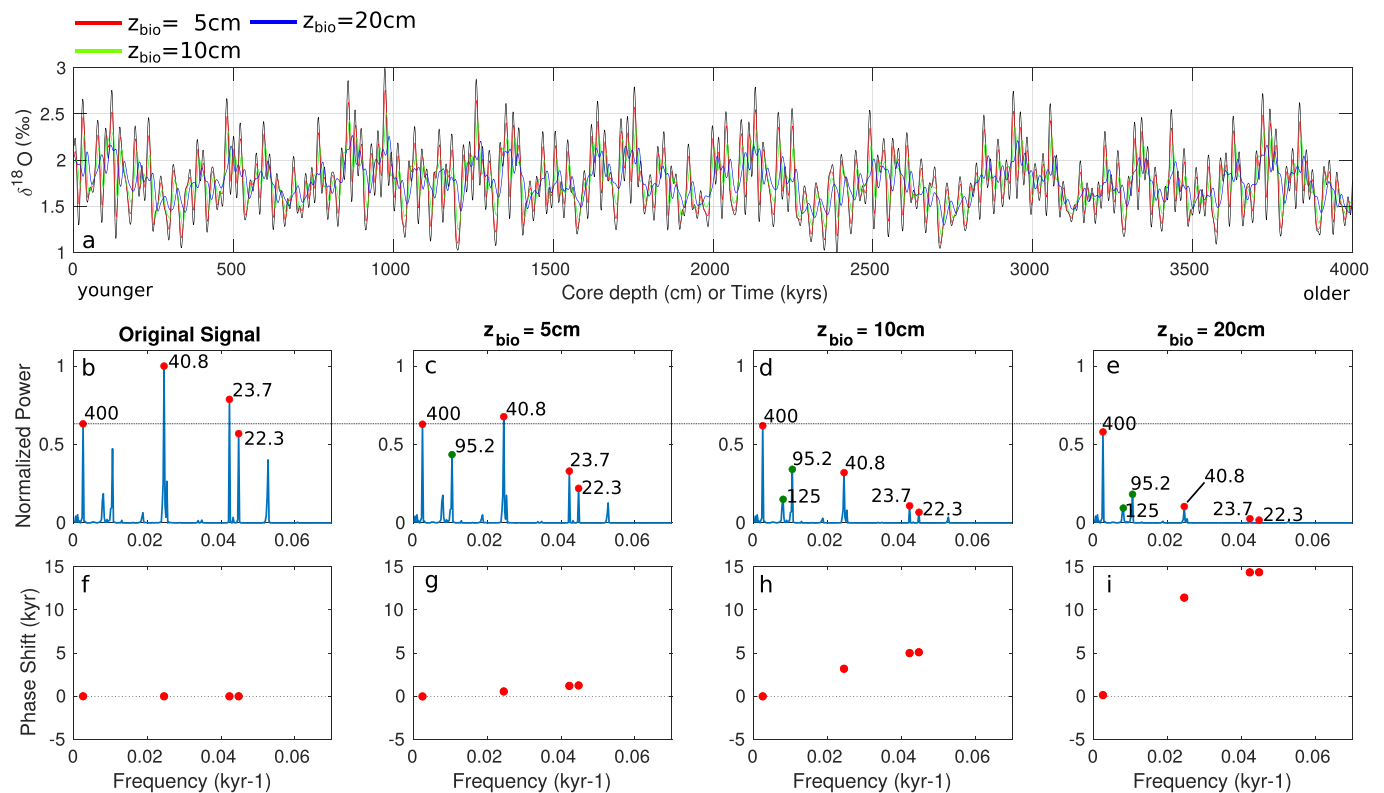


Fig. 7. Homogeneous mixing of an isotopic signal derived from the astronomical solution of [Laskar et al. \(2004\)](#) for the last 4 Million years. a: Time-series of original (black) and bioturbated signals using three different mixed layer depths. b-e: Power spectra of the four signals, normalized to the maximum power of the original signal. The four main frequency-peaks of the original signal are indicated by red circles. Frequencies that become more prominent because of bioturbation, i.e., becoming one of the four main peaks, are indicated by green circles. The numbers represent the respective period in kyrs. f-i: Phase shift of the four main frequencies of the original signal, where positive values represent a corresponding lead of the bioturbated signal relative to the original signal. It is possible to translate sediment core depth into the time domain by assuming a sedimentation rate of 1 cm kyr^{-1} . Note, however, that time here denotes model-time or ‘layer’ age, as the mean age of all particles in a specific layer can be very different due to bioturbation ([Guinasso and Schink, 1975](#)). Power spectra are estimated using periodograms, via Fast Fourier Transform of the modeled time series ([Cooley and Tukey, 1965](#)).

climates. These abundance changes can be species specific. For instance, a warm-adapted, subtropical species will increase in abundance under a warming climate while, at the same time, a cold-adapted, subpolar species will decrease in abundance. To illustrate the influence of these species-specific variations on the measured isotopic signal under bio-mixing, we perform two experiments adapted from [Löwemark et al. \(2008\)](#) and [Trauth \(2013\)](#). In both experiments the bioturbation depth is fixed to 10 cm, and the same transitions between cold and warm climates are simulated - represented by identical abrupt changes between heavy (3.0‰) and light (1.0‰) oxygen isotopes (black lines in [Fig. 9b + d](#)). In the first experiment, we assume these climatic changes are recorded in a warm-adapted foraminifera species. Here, the oxygen isotope change from 3.0‰ to 1.0‰ (i.e., a transition from a cold to a warm climate) is synchronous with an abrupt increase in the warm-adapted species abundance from 100 to 900 particles and vice versa (black lines in [Fig. 9a](#)). In the second experiment, we assume that the same isotopic signal is recorded in a cold-adapted foraminifera species. Here, the same climatic changes (i.e., the same oxygen isotope changes between heavy (3.0‰) and light (1.0‰)) have the reverse effect on the abundance of the cold-adapted species (black lines in [Fig. 9c](#)). In both experiments we choose a smaller sample size of 20 signal carriers that are picked and measured in each layer (i.e., a typical value for planktonic foraminifera). The smaller sample size introduces some additional uncertainty to the recorded isotope signal.

Due to the combined effects of bio-mixing and differential abundance change, the isotopic signals recorded in the two species are notably different ([Fig. 9b + d](#)). The first transition from a cold to a warm climate occurs at a depth of $\sim 180 \text{ cm}$. Due to bio-mixing, the isotope

record in both foraminifera species starts changing at the base of the mixed layer, i.e., $\sim 10 \text{ cm}$ deeper in the sediments ([Fig. 9b + d](#)). However, whereas the isotopic signal measured in the warm-adapted foraminifera changes almost instantaneously, the transition of the signal measured in the cold species extends over $\sim 80 \text{ cm}$, until a value of 1.0‰ is approached (compare [Fig. 9b + d](#)). The second climate transition from a warm to a cold climate at $\sim 105 \text{ cm}$ is documented analogously. The cold-adapted species now displays the instantaneous isotopic exchange, as its abundance is simultaneously enhanced. The second isotope excursion to 1.0‰ between $\sim 65\text{--}75 \text{ cm}$ is expressed differently in the two foraminifera species. The warm-adapted species displays an oxygen isotopic excursion to almost 1.0‰ ([Fig. 9b](#)), while the cold-adapted species only displays an isotopic excursion to $\sim 2.7\text{‰}$ ([Fig. 9d](#)). The much larger isotopic excursion recorded in the warm-adapted species has two causes. First, its isotopic signal has not fully recovered to 3.0‰ before the second climate warming event starts. Second, the transition to light oxygen isotopes is recorded almost instantaneously in the warm-adapted species because of the simultaneous increase in abundance.

4.2.2. ‘Real’ world example - $\delta^{13}\text{C}$ records from ODP Site 690

Finally, we use *iTURBO2* to simulate the combined effects of bioturbation and differential abundance change on single-foraminifera isotope records. For this, we use the high-resolution, single-foraminifera stable isotope records of mixed layer and thermocline-dwelling planktonic foraminifera from Ocean Drilling Program (ODP) Site 690 in the Southern Ocean ([Thomas et al., 2002](#)). Although these records have been pivotal to our understanding of the PETM, the lack of intermediate isotopic values and the large stratigraphic offset ($\sim 8 \text{ cm}$)

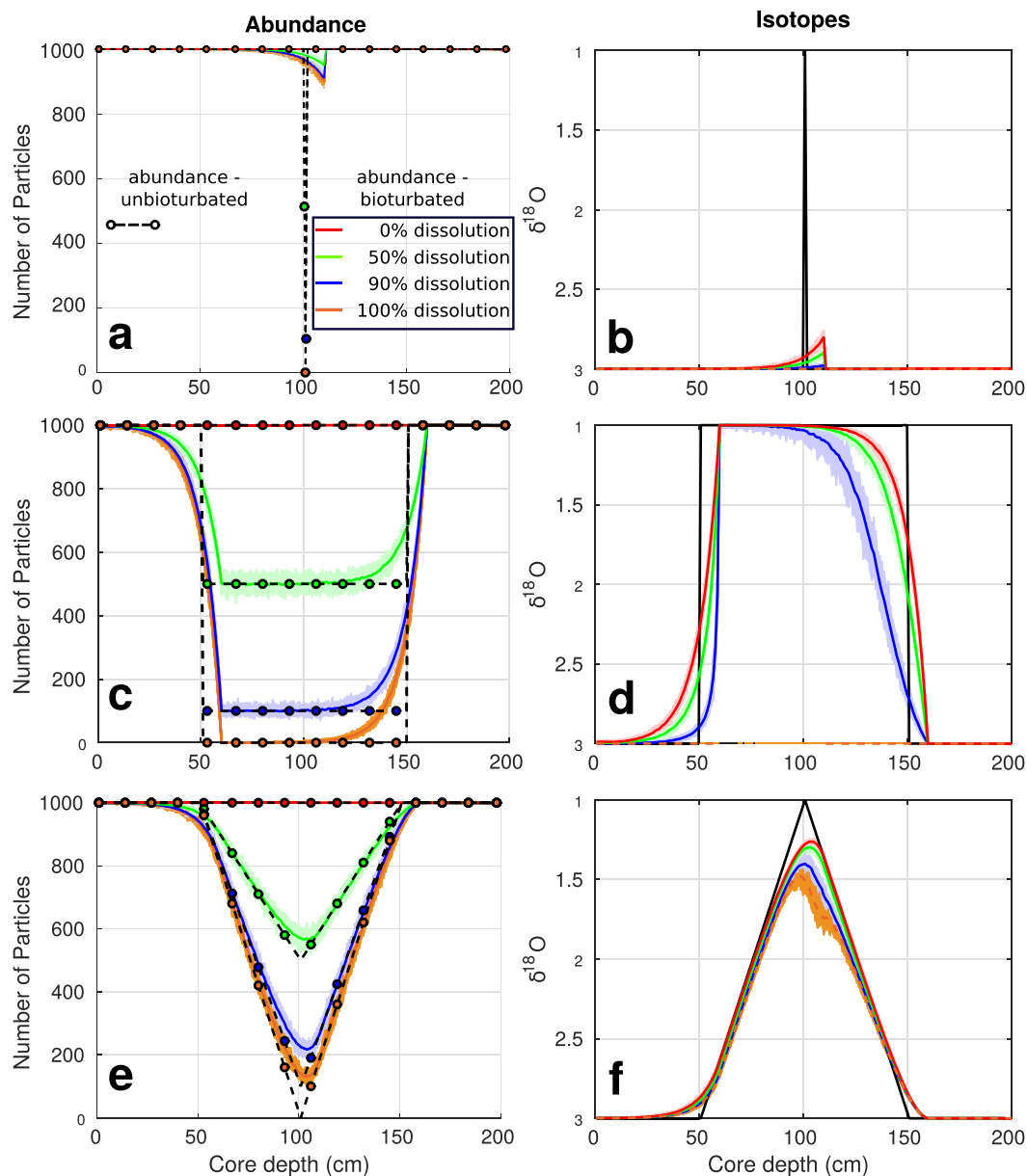


Fig. 8. Sediment records created by co-varying foraminifera abundance and isotopic signal. Left column: Dashed lines showing the abundance change applied to the sediment column before bioturbational mixing. Coloured lines represent the abundance after applying bioturbational mixing in the upper 10 cm. The four colours represent the different abundance-change scenarios. Right column: Black lines are the idealized isotopic changes applied, as in Table 1, before bioturbational mixing. The coloured lines represent the measured, bioturbated isotopic signals for the four abundance-change scenarios.

between the isotopic excursions initiated in the two different foraminifera species (Fig. 10a) has remained enigmatic for a long time; however, new evidence suggests that sediment mixing can explain these observations (Kirtland Turner et al., 2017; Hupp et al., 2019).

In the following, we show how idealized isotopic and abundance changes even in the simple *i*TURBO2 model framework can help explain the large stratigraphic offset between the carbon isotopic excursions. To do so, we adapted the approach of Kirtland Turner et al. (2017), who employed the Lagrangian mixing model of Hull et al. (2011). We assume a homogeneously mixed layer of 10 cm and a sedimentation rate of 2.5 cm kyr⁻¹, which is typical at this site during the late Paleocene (e.g. Farley and Eltgroth, 2003; Röhl et al., 2007). We assume an instantaneous step change in the carbon isotopic values of both species, coincident with the onset of the carbon-isotope excursion (CIE). Following Kirtland Turner et al. (2017) and based on ODP Site 690 data (Thomas et al., 2002), mixed layer foraminifera were assigned a mean pre-event

$\delta^{13}\text{C}$ value of 3.1‰ and a mean CIE value of 0.0‰, with a standard deviation of 0.3‰. Thermocline foraminifera were assigned a mean pre-event $\delta^{13}\text{C}$ value of 1.6‰ and a mean CIE value of -0.4‰, with a standard deviation of 0.12‰. Coincident with the CIE, large shifts in the population of planktonic foraminifera occurred. Mixed-layer and thermocline taxa exhibit pronounced fluctuations in relative abundance (Kelly, 2002). To simulate these observed changes with *i*TURBO2, we reduce the initial abundance (10,000 each species) of the mixed-layer and the thermocline taxa throughout the sediment column. We reduce the mixed-layer taxa to 50%, and the thermocline taxa to 0.1% for the first 10 cm and subsequently to 1% of their initial abundance. We simulate the abundance changes as a single step, simultaneous with the onset of the CIE (Fig. 10d).

We ran *i*TURBO2 for the mixed-layer and the thermocline species and simulated 10,000 individual sediment particles in every sediment layer for each experiment. For direct comparison to isotopic

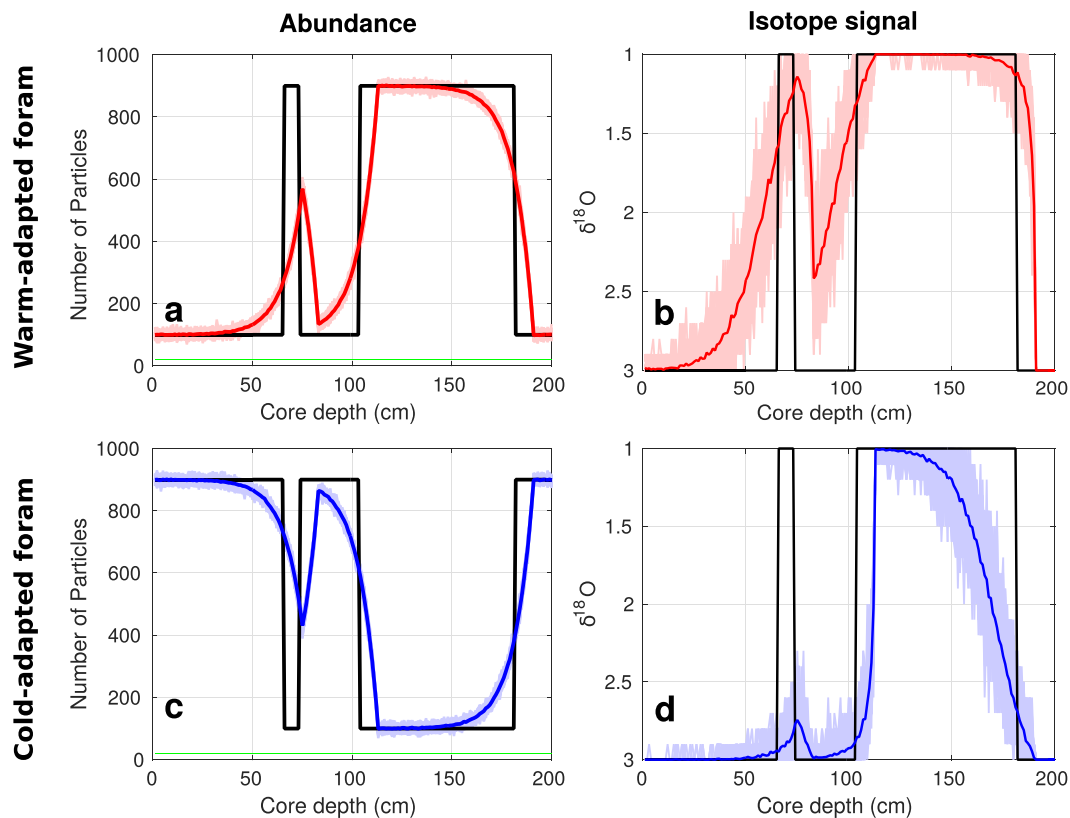


Fig. 9. Measured isotopic signals for two foraminifera species with opposite abundance changes in response to the same climate variations (here transitions from warm to cold climates and vice versa). Top in red: warm-adapted foraminifera records. Bottom in blue: cold-adapted foraminifera records. For instance, the abundance of the warm-adapted species increases from 100 to 900 simultaneously with a shift from a cold to a warm climate (represented by a change from heavy to light isotopes, black lines represent the original abundance and isotope changes). The resulting isotopic signals measured in the two species are significantly different (colored lines in b + d). The green lines in (a + c) show the number of particles picked per sediment layer, here 20.

observations (Thomas et al., 2002), we randomly selected $n = 4$ individuals from each of the two depth habitat groups every 2.5 cm from the theoretical sediment columns produced by *i*TURBO2. To investigate the effect of using a larger sampling size, we additionally select $n = 12$ individuals. Because of the stochastic nature of the model and random selection of individuals every 2.5 cm, each model run results in slightly different single-foraminifera isotopic patterns, for which Fig. 10b and c provide examples.

The simplified (10 cm homogeneous layer) mixing scenario produces single-specimen carbon-isotope records comparable to the observed data from ODP Site 690 (Fig. 10b, c). The combined effects of bioturbation, unequal abundance changes, and small sample size in *i*TURBO2 can, thus, readily explain the offset between the $\delta^{13}\text{C}$ excursion observed in mixed-layer and thermocline dwellers. Using a larger sample size of $n = 12$ does not decrease the observed stratigraphic offset between the onset of the CIE in the two different foraminifera species. On the contrary, it can make the offset appear even larger, due to the higher probability of picking/recording a foraminiferal test in a deeper pre-CIE layer that was remobilized by bioturbation from the CIE.

5. Conclusions and perspectives

We have provided an overview of different numerical approaches to simulate the effects of bioturbational mixing on the sedimentary record. The models can be mechanistically divided into continuum models and explicit particle models, each having different applications. Continuum models are generally applied to study bulk sediment movement and simulate tracer concentration profiles. Explicit particle models simulate the movement of individual sediment particles and can be used for direct comparison with paleoclimate single-specimen signals.

We apply a simple explicit particle model to illustrate some of the well-known effects of bioturbation, i.e., altering of timing, duration, and magnitude of a paleo-event, for a set of conceptual proxy profile shapes. Our results show that deep bioturbation strongly obscures the apparent magnitude and duration of all conceptual proxy records. Furthermore, we demonstrate that bioturbation induces unequal shifts in spectral power and phase of an orbitally mediated isotopic signal. Longer eccentricity-like cycles gain relative power and experience only small phase-shifts, while short precession-like cycles almost disappear and experience large phase-shifts. This so-called low-pass filtering effect clearly hinders the interpretation of longer marine isotopic records and complicates their correlation with non-bioturbated signals, with important implications for cyclostratigraphy.

In addition, we illustrate some of the perhaps less well-known effects of bioturbation, such as the errors induced in sampled isotopic records arising from mixing and unequal fluctuations in foraminifera abundance, which can occur due to differential species-specific responses to environmental changes. We show that isotope records from two different foraminifera species with changing relative abundances in the same core can result in significant discrepancies in the timing and magnitude of events due to bioturbational mixing. It is, therefore, important to be aware of relative abundance changes, as well as post-depositional alterations. Ideally, a predominant species with relatively low abundance fluctuations should be used for single-specimen isotopic data. Clearly, signals from sediment layers with low foraminifera abundance should be interpreted very carefully, as they are likely biased by specimens from layers with higher abundance.

What we have not illustrated here are further complications arising from (partial or complete) dissolution – which may be particle (species) specific, particle size-dependent mixing, or the precipitation of

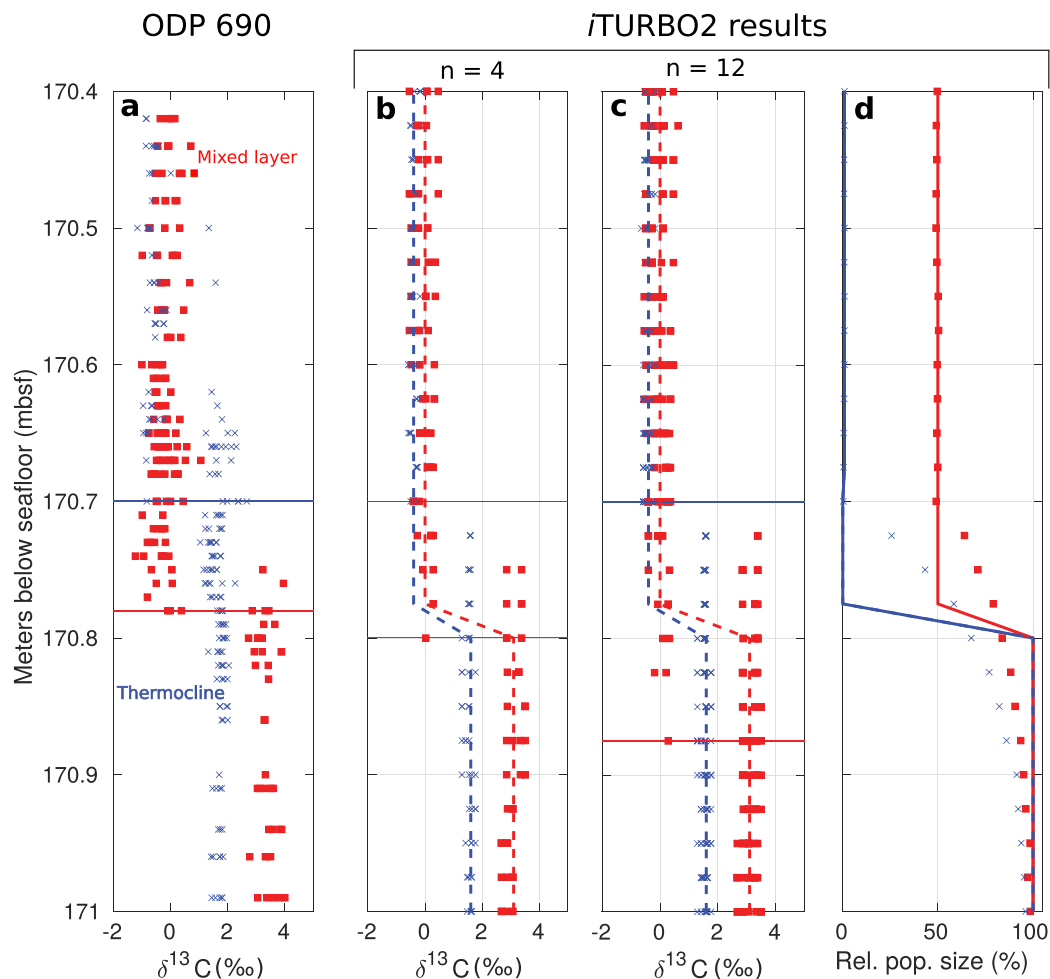


Fig. 10. *iTURBO2* simulations with differential abundance changes between mixed-layer and thermocline taxa can explain patterns in ODP Site 690 data. **a:** Single-foraminifera isotope data from ODP Site 690 across the PETM from mixed-layer (red) and thermocline (blue) dwelling foraminifera $\delta^{13}\text{C}$ (data from [Thomas et al., 2002](#)). **b, c:** *iTURBO2* simulations of $\delta^{13}\text{C}$ in mixed-layer (red) and thermocline (blue) taxa assuming a greater change in the abundance of the thermocline species using sample sizes of $n = 4$ individuals (**b**) and $n = 12$ (**c**). Dashed lines represent the original, unmixed signal. **d:** Simulated abundance changes where lines represent the unmixed abundance and symbols the post-mixing abundance. The simulated instantaneous onset of the carbon isotope excursion (CIE) and the abundance change in the unmixed record occurs in all groups simultaneously at 170.8 mbsf.

secondary authigenic phases with differing proxy (e.g., isotopic) signatures compared to the primary phase. While *iTURBO2* could be adapted to explore the effects of size-dependent mixing, a meaningful representation of dissolution and re-precipitation requires a geochemical reactive-transport approach. The nature (e.g., frequency, depth) of bioturbation may also not be static but instead co-vary with environmental factors such as bottom water oxygenation and food (organic matter) availability, and in the geological record may be impacted by extinction (e.g., PETM, [Thomas, 2003](#)). As discussed earlier, spatially resolved models (or packets of particles), geochemical reactions, and even environment-dependent animal behavior and activity do exist (e.g., *iLABS*, [Kanzaki et al., 2019](#)) but can be numerically very expensive. For instance, simulating 10 years in *iLABS* takes about seven days of CPU time, whereas the simpler *LABS* model can simulate 10 years in less than one CPU hour. As an alternative, compromises and simplifications can be used, such as parameterizing biodiffusion as a function of oxygenation and food availability (e.g., [Muds; Archer et al., 2002](#)), and for many simple problems, fixed biodiffusion approaches of bulk sediment performs well ([Soetaert et al., 1996](#); [Meysman et al., 2010](#)). However, analytical technology pushes towards ever smaller samples, and single-particle (e.g., foram) analysis becomes more common. Therefore, particle-resolving models (ideally accounting for size-dependent mixing and species- and size-dependent dissolution) are

indispensable for quantifying the effects of bioturbation on the recorded signal. Novel models building on approaches such as ‘IMP’ ([Kanzaki et al., 2021](#)) that combine a 1-D reaction-transport framework with particles (or packets of particles) that run efficiently are needed, and should be accessible for a wider community for routine use and exploration.

iLABS arguably constitutes the most comprehensive encapsulation of bioturbational mixing to date. Further developments to include more ecological aspects could improve the model’s realism and potentially lead to non-diffusive bioturbational mixing. For instance, the life cycle and the size of bioturbators (and their ‘offspring’) could be implemented as a function of oxygen levels and food availability. The death of organisms could be related to low oxygen concentrations or the presence of a toxic tracer, such as hydrogen sulfide. Thus, the organisms’ morphological properties and behavior would be affected by ecological changes, enabling a more meaningful comparison of *iLABS* results with the ichnological and taphonomical sediment records. Such ecology-enabled diagenetic/bioturbation models might help to better understand trace fossils in the geological record.

Finally, we would like to point out that this paper has only discussed and illustrated forward-modeling approaches to explore how bioturbation encodes primary environmental signals into the geological record. The ability to un-mix recovered records is something of a holy

grail of paleoclimate and may require the application of simplified continuum models, which allow explicit deconvolution, as well as further innovations, perhaps involving Monte Carlo simulation and/or deep learning, as well as multi-proxy constraints. Generally, the scientific question should determine the complexity of the model to be used. Continuum and explicit particle models may also be used in combination to provide a deeper understanding. In the absence of formal ways of recovering the primary signal, awareness of how signals can be distorted is key, as is the ability to experiment with how different primary signals might give rise to the observed outcome.

Code availability

The iTURBO2 code used in this paper is tagged as v1.0 and is available at <https://doi.org/10.5281/zenodo.6669565>. The source code is hosted on GitHub and can be obtained by cloning <https://github.com/imuds/iTURBO2>. Details of the experiments, plus the command line needed to run each one, are given in the README.txt file in that directory. All other boundary condition files are provided as part of the code release.

Declaration of Competing Interest

The authors declare that they have no known competing financial interests or personal relationships that could have appeared to influence the work reported in this paper.

Data availability

See 'Code Availability' section for information on how to access the code.

Acknowledgments

This paper arose from a workshop on "Instigating a Mechanistic Understanding of the Dynamics of the Sedimentary record ('iMUDS')" that was sponsored by the Heising-Simons foundation. We would like to thank Stephen Meyers (UW-Madison) and three anonymous reviewers for their constructive critiques and suggestions that have improved this paper. We thank Martin Trauth for developing the original TURBO2 model. DH is supported by a postdoctoral fellowship from the Simons Foundation (Award 653829). SJV is supported by the Belgian Science Policy office (BELSPO, Grant No. FED-tWIN2019-prf-008). DH, PV, YK, AR and SKT acknowledge support from the Heising-Simons Foundation (Grant No. #2015–145). BH acknowledges support from UKRI Future Leaders GrantMR/S034293/1. MK and JJM thank support from the Netherlands Earth System Science Centre financially supported by the Ministry of Education, Culture and Science (OCW).

References

Alegret, L., Rodríguez-Tovar, F.J., Uchman, A., 2015. How bioturbation obscured the Cretaceous-Palaeogene boundary record. *Terra Nova* 27 (3), 225–230.

Aller, R.C., 1982. The Effects of Macrobenthos on Chemical Properties of Marine Sediment and Overlying Water. In: McCall, P.L., Tevesz, M.J.S. (Eds.), *Animal-Sediment Relations: The Biogenic Alteration of Sediments*, Topics in Geobiology. Springer, US, Boston, MA, pp. 53–102.

Anderson, D.M., 2001. Attenuation of millennial-scale events by bioturbation in marine sediments. *Paleoceanography* 16 (4), 352–357.

Archer, D.E., Morford, J.L., Emerson, S.R., 2002. A model of suboxic sedimentary diagenesis suitable for automatic tuning and gridded global domains. *Global Biogeochem. Cycles* 16 (1), 17–1.

Ausich, W.I., Bottjer, D.J., 1982. Tiering in Suspension-Feeding Communities on Soft Substrata Throughout the Phanerozoic. *Science* 216 (4542), 173–174.

Bambach, R.K., 1993. Seafood through time: changes in biomass, energetics, and productivity in the marine ecosystem. *Paleobiology* 19 (3), 372–397.

Bao, R., Blattmann, T.M., McIntyre, C., Zhao, M., Eglinton, T.I., 2019. Relationships between grain size and organic carbon 14C heterogeneity in continental margin sediments. *Earth Planet. Sci. Lett.* 505, 76–85.

Bard, E., 2001. Paleoceanographic implications of the difference in deep-sea sediment mixing between large and fine particles. *Paleoceanography* 16 (3), 235–239.

Bard, E., Arnold, M., Duprat, J., Moyes, J., Duplessy, J.-C., 1987. Reconstruction of the last deglaciation: deconvolved records of $\delta^{18}\text{O}$ profiles, micropaleontological variations and accelerator mass spectrometric 14C dating. *Clim. Dyn.* 1 (2), 101–112.

Berger, W.H., 1968. Planktonic Foraminifera: selective solution and paleoclimatic interpretation. *Deep Sea Res. Oceanogr. Abstr.* 15 (1), 31–43.

Berger, W.H., Heath, G.R., 1968. Vertical Mixing in Pelagic Sediments. *J. Mar. Res.* 26, 134–143.

Berger, W.H., Johnson, R.F., Killingley, J.S., 1977. 'Unmixing' of the deep-sea record and the deglacial meltwater spike. *Nature* 269 (5630), 661.

Berner, R.A., Westrich, J.T., 1985. Bioturbation and the early diagenesis of carbon and sulfur. *Am. J. Sci.; (United States)* 1, 3.

Biles, C.L., Paterson, D.M., Ford, R.B., Solan, M., Raffaelli, D.G., 2002. Bioturbation, ecosystem functioning and community structure. *Hydrol. Earth Syst. Sci. Discuss.* 6 (6), 999–1005.

Boudreau, B.P., 1986. Mathematics of tracer mixing in sediments; I, Spatially-dependent, diffusive mixing. *Am. J. Sci.* 286 (3), 161–198.

Boudreau, B.P., 1998. Mean mixed depth of sediments: the wherefore and the why. *Limnol. Oceanogr.* 43 (3), 524–526.

Boudreau, B.P., 2004. What controls the mixed-layer depth in deep-sea sediments? The importance of particulate organic carbon flux. *Limnol. Oceanogr.* 49 (2), 620–622.

Boudreau, B.P., Imboden, D.M., 1987. Mathematics of tracer mixing in sediments; III, The theory of nonlocal mixing within sediments. *Am. J. Sci.* 287 (7), 693–719.

Broecker, W.S., Clark, E., 1999. CaCO_3 size distribution: a paleocarbonate ion proxy? *Paleoceanography* 14 (5), 596–604.

Broecker, W.S., Clark, E., 2001. Reevaluation of the CaCO_3 size index paleocarbonate ion proxy. *Paleoceanography* 16 (6), 669–671.

Bromley, R.G., 2012. Trace fossils: biology, taxonomy and applications. Routledge.

Brown, L., Cook, G.T., MacKenzie, A.B., Thomson, J., 2001. Radiocarbon Age Profiles and Size Dependency of Mixing in Northeast Atlantic Sediments. *Radiocarbon* 43 (2B), 929–937.

Cadée, G.C., 2001. Sediment Dynamics by Bioturbating Organisms. In: Reise, K. (Ed.), *Ecological Comparisons of Sedimentary Shores*, Ecological Studies. Springer, Berlin, Heidelberg, pp. 127–148.

Choi, J., Francois-Carcaillet, F., Boudreau, B.P., 2002. Lattice-automaton bioturbation simulator (LABS): implementation for small deposit feeders. *Comput. Geosci.* 28 (2), 213–222.

Cobain, S.L., Hodgson, D.M., Peakall, J., Wignall, P.B., Cobain, M.R.D., 2018. A new macrofaunal limit in the deep biosphere revealed by extreme burrow depths in ancient sediments. *Sci. Rep.* 8 (1).

Cochran, J.K., 1985. Particle mixing rates in sediments of the eastern equatorial Pacific: Evidence from 210Pb, 239,240Pu and 137Cs distributions at MANOP sites. *Geochim. Cosmochim. Acta* 49 (5), 1195–1210.

Cooley, J.W., Tukey, J.W., 1965. An Algorithm for the Machine Calculation of Complex Fourier Series. *Math. Comput.* 19 (90), 297–301. Publisher: American Mathematical Society.

Coulbourn, W.T., Parker, F.L., Berger, W.H., 1980. Faunal and solution patterns of planktonic foraminifera in surface sediments of the North Pacific. *Mar. Micropaleontol.* 5, 329–399.

Crimes, T.P., Droser, M.L., 1992. Trace Fossils and Bioturbation: The Other Fossil Record. *Annu. Rev. Ecol. Syst.* 23, 339–360. Publisher: Annual Reviews.

Curry, W.B., Oppo, D.W., 2005. Glacial water mass geometry and the distribution of $\delta^{13}\text{C}$ of ΣCO_2 in the western Atlantic Ocean. *Paleoceanography* 20 (1).

Dorgan, K.M., Jumars, P.A., Johnson, B., Boudreau, B.P., Landis, E., 2005. Burrow extension by crack propagation. *Nature* 433, 475–475.

Dorgan, K.M., Jumars, P.A., Johnson, B.D., Boudreau, B.P., 2006. Macrofaunal burrowing: the medium is the message. *Oceanogr. Mar. Biol.* 44, 85–121.

Eglinton, T.I., Eglinton, G., 2008. Molecular proxies for paleoclimatology. *Earth Planet. Sci. Lett.* 275 (1), 1–16.

Elderfield, H., Ganssen, G., 2000. Past temperature and $\delta^{18}\text{O}$ of surface ocean waters inferred from foraminiferal Mg/Ca ratios. *Nature* 405 (6785), 442–445.

Esmeray-Senlet, S., Miller, K.G., Sherrell, R.M., Senlet, T., Vellekoop, J., Brinkhuis, H., 2017. Iridium profiles and delivery across the Cretaceous/Paleogene boundary. *Earth Planet. Sci. Lett.* 457, 117–126.

Farley, K.A., Eltgroth, S.F., 2003. An alternative age model for the Paleocene-Eocene thermal maximum using extraterrestrial ^3He . *Earth Planet. Sci. Lett.* 208 (3), 135–148.

Field, D.B., Baumgartner, T.R., Charles, C.D., Ferreira-Bartrina, V., Ohman, M.D., 2006. Planktonic Foraminifera of the California Current Reflect 20th-Century Warming. *Science* 311 (5757), 63–66.

Foster, D.W., 1985. BIOTURB: A FORTRAN program to simulate the effects of bioturbation on the vertical distribution of sediment. *Comput. Geosci.* 11 (1), 39–54.

Foster, G.L., Rae, J.W., 2016. Reconstructing Ocean pH with Boron Isotopes in Foraminifera. *Annu. Rev. Earth Planet. Sci.* 44 (1), 207–237.

François, F., Poggiale, J.-C., Durbec, J.-P., Stora, G., 1997. A New Approach for the Modelling of Sediment Reworking Induced by a Macrobenthic Community. *Acta. Biotheor.* 45 (3), 295–319.

Gardner, L.R., Sharma, P., Moore, W.S., 1987. A regeneration model for the effect of bioturbation by fiddler crabs on 210Pb profiles in salt marsh sediments. *J. Environ. Radioact.* 5 (1), 25–36.

Glass, B.P., 1969. Reworking of deep-sea sediments as indicated by the vertical dispersion of the Australasian and ivory coast microtektite horizons. *Earth Planet. Sci. Lett.* 6 (6), 409–415.

- Goldberg, E.D., Koide, M., 1962. Geochronological studies of deep sea sediments by the ionium/thorium method. *Geochim. Cosmochim. Acta* 26 (3), 417–450.
- Goreau, T.J., 1980. Frequency sensitivity of the deep-sea climatic record. *Nature* 287 (5783), 620–622.
- Gougeon, R.C., Mángano, M.G., Buatois, L.A., Narbonne, G.M., Laing, B.A., 2018. Early Cambrian origin of the shelf sediment mixed layer. *Nat. Commun.* 9 (1), 1909.
- Green, M.A., Aller, R.C., Cochran, J.K., Lee, C., Aller, J.Y., 2002. Bioturbation in shelf/slope sediments off Cape Hatteras, North Carolina: the use of ²³⁴Th, Chl-a, and Br- to evaluate rates of particle and solute transport. *Deep Sea Res. Part II* 49 (20), 4627–4644.
- Guinasso, N.L., Schink, D.R., 1975. Quantitative estimates of biological mixing rates in abyssal sediments. *J. Geophys. Res.* 80 (21), 3032–3043.
- Henderson, G.M., 2002. New oceanic proxies for paleoclimate. *Earth Planet. Sci. Lett.* 203 (1), 1–13.
- Hendy, I.L., Kennett, J.P., 2000. Dansgaard-Oeschger Cycles and the California Current System: Planktonic foraminiferal response to rapid climate change in Santa Barbara Basin, Ocean Drilling Program Hole 893A. *Paleoceanography* 15 (1), 30–42.
- Hillaire-Marcel, C., Vernal, A., 2007. Proxies in Late Cenozoic Paleocyanography. Elsevier.
- Hönisch, B., Eggins, S.M., Haynes, L.L., Allen, K.A., Holland, K.D., Lorbacher, K., 2019. Boron Proxies in Paleocyanography and Paleoclimatology. John Wiley & Sons.
- Hoogakker, B.A.A., Elderfield, H., Schmiedl, G., McCave, I.N., Rickaby, R.E.M., 2015. Glacial–interglacial changes in bottom-water oxygen content on the Portuguese margin. *Nat. Geosci.* 8 (1), 40–43. Publisher: Nature Publishing Group.
- Hull, P.M., Franks, P.J.S., Norris, R.D., 2011. Mechanisms and models of iridium anomaly shape across the Cretaceous–Paleogene boundary. *Earth Planet. Sci. Lett.* 301 (1), 98–106.
- Hupp, B.N., Kelly, D.C., Zachos, J.C., Bralower, T.J., 2019. Effects of size-dependent sediment mixing on deep-sea records of the Paleocene-Eocene Thermal Maximum. *Geology* 47 (8), 749–752.
- Hutson, W.H., 1980. Bioturbation of deep-sea sediments: oxygen isotopes and stratigraphic uncertainty. *Geology* 8 (3), 127–130.
- Hülse, D., Arndt, S., Daines, S., Regnier, P., Ridgwell, A., 2018. OMEN-SED 1.0: a novel, numerically efficient organic matter sediment diagenesis module for coupling to Earth system models. *Geosci. Model Dev.* 11 (7), 2649–2689.
- Jorissen, F.J., Fontanier, C., Thomas, E., 2007. Chapter seven paleoceanographical proxies based on deep-sea benthic foraminiferal assemblage characteristics. *Dev. Mar. Geol.* 1, 263–325.
- Kanzaki, Y., Boudreau, B.P., Kirtland Turner, S., Ridgwell, A., 2019. A lattice-automaton bioturbation simulator with coupled physics, chemistry, and biology in marine sediments (eLABS v0.2). *Geosci. Model Dev.* 12 (10), 4469–4496.
- Kanzaki, Y., Hülse, D., Kirtland Turner, S., Ridgwell, A., 2021. A model for marine sedimentary carbonate diagenesis and paleoclimate proxy signal tracking: IMP v1.0. *Geosci. Model Dev.* 14 (10), 5999–6023.
- Kelly, D.C., 2002. Response of Antarctic (ODP Site 690) planktonic foraminifera to the Paleocene-Eocene thermal maximum: Faunal evidence for ocean/climate change. *Paleoceanography* 17 (4), 231–233.
- Kirtland Turner, S., Hull, P.M., Kump, L.R., Ridgwell, A., 2017. A probabilistic assessment of the rapidity of PETM onset. *Nat. Commun.* 8 (1), 1–10.
- Kirtland Turner, S., Ridgwell, A., 2013. Recovering the true size of an Eocene hyperthermal from the marine sedimentary record. *Paleoceanography* 28 (4), 2013PA002541.
- Kristensen, E., Penha-Lopes, G., Delefosse, M., Valdemarsen, T., Quintana, C.O., Banta, G. T., 2012. What is bioturbation? The need for a precise definition for fauna in aquatic sciences. *Mar. Ecol. Prog. Ser.* 446, 285–302.
- Kucera, M., 2007. Chapter Six Planktonic Foraminifera as Tracers of Past Oceanic Environments. In: Hillaire-Marcel, C., De Vernal, A. (Eds.), *Developments in Marine Geology, Proxies in Late Cenozoic Paleocyanography*, vol. 1. Elsevier, pp. 213–262.
- Laskar, J., Robutel, P., Joutel, F., Gastineau, M., Correia, A.C.M., Levrard, B., 2004. A long-term numerical solution for the insolation quantities of the Earth. *Astron. Astrophys.* 428 (1), 261–285.
- Lau, K.V., Romaniello, S.J., Zhang, F., 2019. The Uranium Isotope Paleoredox Proxy. *Elements in Geochemical Tracers in Earth System Science*.
- Lea, D.W., Boyle, E.A., 1990. A 210,000-year record of barium variability in the deep northwest Atlantic Ocean. *Nature* 347 (6290), 269.
- Levinton, J., 1995. Bioturbators as Ecosystem Engineers: Control of the Sediment Fabric, Inter-Individual Interactions, and Material Fluxes. In: Jones, C.G., Lawton, J.H. (Eds.), *Linking Species & Ecosystems*. Springer, US, Boston, MA, pp. 29–36.
- Liu, H., Meyers, S.R., Marcott, S.A., 2021. Unmixing deep-sea paleoclimate records: a study on bioturbation effects through convolution and deconvolution. *Earth Planet. Sci. Lett.* 564, 116883.
- Lougheed, B.C., 2020. SEAMUS (v1.20): a $\Delta^{14}\text{C}$ -enabled, single-specimen sediment accumulation simulator. *Geosci. Model Dev.* 13 (1), 155–168.
- Lougheed, B.C., Metcalfe, B., 2022. Testing the effect of bioturbation and species abundance upon discrete-depth individual foraminifera analysis. *Biogeosciences* 19 (4), 1195–1209.
- Lourens, L.J., Sluijs, A., Kroon, D., Zachos, J.C., Thomas, E., Röhl, U., Bowles, J., Raffi, I., 2005. Astronomical pacing of late Paleocene to early Eocene global warming events. *Nature* 435 (7045), 1083–1087.
- Löwemark, L., Konstantinou, K.I., Steinke, S., 2008. Bias in foraminiferal multispecies reconstructions of paleohydrographic conditions caused by foraminiferal abundance variations and bioturbational mixing: a model approach. *Mar. Geol.* 256 (1), 101–106.
- Maire, O., Lecroart, P., Meysman, F., Rosenberg, R., Duchêne, J.-C., Grémare, A., 2008. Quantification of sediment reworking rates in bioturbation research: a review. *Aquat. Biol.* 2 (3), 219–238.
- McIlroy, D., 2008. Ichnological analysis: The common ground between ichnofacies workers and ichnofabric analysts. *Palaeogeogr. Palaeoclimatol. Palaeoecol.* 270 (3), 332–338.
- Meile, C., Van Cappellen, P., 2005. Particle age distributions and O₂ exposure times: timescales in bioturbated sediments. *Global Biogeochem. Cycles* 19 (3).
- Metcalfe, B., Lougheed, B.C., Waelbroeck, C., Roche, D.M., 2020. A proxy modelling approach to assess the potential of extracting ENSO signal from tropical Pacific planktonic foraminifera. *Clim. Past* 16 (3), 885–910. Publisher: Copernicus GmbH.
- Meyers, P.A., 1997. Organic geochemical proxies of paleoceanographic, paleolimnologic, and paleoclimatic processes. *Org. Geochem.* 27 (5), 213–250.
- Meysman, F.J.R., Boudreau, B.P., Middelburg, J.J., 2003. Relations between local, nonlocal, discrete and continuous models of bioturbation. *J. Mar. Res.* 61 (3), 391–410.
- Meysman, F.J.R., Boudreau, B.P., Middelburg, J.J., 2010. When and why does bioturbation lead to diffusive mixing? *J. Mar. Res.* 68 (6), 881–920.
- Meysman, F.J.R., Malyuga, V.S., Boudreau, B.P., Middelburg, J.J., 2008a. A generalized stochastic approach to particle dispersal in soils and sediments. *Geochim. Cosmochim. Acta* 72 (14), 3460–3478.
- Meysman, F.J.R., Malyuga, V.S., Boudreau, B.P., Middelburg, J.J., 2008b. Quantifying particle dispersal in aquatic sediments at short time scales: model selection. *Aquat. Biol.* 2 (3), 239–254.
- Meysman, F.J.R., Middelburg, J.J., Heip, C.H.R., 2006. Bioturbation: a fresh look at Darwin's last idea. *Trends Ecol. Evol.* 21 (12), 688–695.
- Moffitt, S.E., Moffitt, R.A., Sauthoff, W., Davis, C.V., Hewett, K., Hill, T.M., 2015. Paleocyanographic Insights on Recent Oxygen Minimum Zone Expansion: Lessons for Modern Oceanography. *PLoS One* 10 (1), e0115246. Publisher: Public Library of Science.
- Morey, A.E., Mix, A.C., Pisias, N.G., 2005. Planktonic foraminiferal assemblages preserved in surface sediments correspond to multiple environment variables. *Quatern. Sci. Rev.* 24 (7), 925–950.
- Pemberton, G.S., Risk, M.J., Buckley, D.E., 1976. Supershrimp: Deep Bioturbation in the Strait of Canso, Nova Scotia. *Science* 192 (4241), 790–791. Publisher: American Association for the Advancement of Science.
- Petit, J.R., Jouzel, J., Raynaud, D., Barkov, N.I., Barnola, J.-M., Basile, I., Bender, M., Chappellaz, J., Davis, M., Delaygue, G., Delmotte, M., Kotlyakov, V.M., Legrand, M., Lipenkov, V.Y., Lorius, C., Pépin, L., Ritz, C., Saltzman, E., Stievenard, M., 1999. Climate and atmospheric history of the past 420,000 years from the Vostok ice core, Antarctica. *Nature* 399 (6735), 429–436.
- Pisias, N.G., 1983. Geologic time series from deep-sea sediments: time scales and distortion by bioturbation. *Mar. Geol.* 51 (1), 99–113.
- Rae, J.W.B., Foster, G.L., Schmidt, D.N., Elliott, T., 2011. Boron isotopes and B/Ca in benthic foraminifera: proxies for the deep ocean carbonate system. *Earth Planet. Sci. Lett.* 302 (3), 403–413.
- Reed, D.C., Boudreau, B.P., Huang, K., 2007. Transient tracer dynamics in a lattice-automaton model of bioturbation. *J. Mar. Res.* 65 (6), 813–833.
- Reed, D.C., Huang, K., Boudreau, B.P., Meysman, F.J.R., 2006. Steady-state tracer dynamics in a lattice-automaton model of bioturbation. *Geochim. Cosmochim. Acta* 70 (23), 5855–5867.
- Reichert, G.-J., Jorissen, F., Anschutz, P., Mason, P.R., 2003. Single foraminiferal test chemistry records the marine environment. *Geology* 31 (4), 355–358.
- Rhoads, D.C., 1974. Organism-sediment relations on the muddy sea floor. *Oceanogr. Mar. Biol.* 12, 263–300.
- Richter, R., 1952. Fluidal-textur in Sediment-Gesteinen und ober sedifikation überhaupt. *Notizbl Hess L-Amt Bodenforsch.* 3, 67–81.
- Robbins, J.A., McCall, P.L., Fisher, J.B., Krezoski, J.R., 1979. Effect of deposit feeders on migration of ¹³⁷Cs in lake sediments. *Earth Planet. Sci. Lett.* 42 (2), 277–287.
- Roche, D.M., Waelbroeck, C., Metcalfe, B., Caley, T., 2018. FAME (v1.0): a simple module to simulate the effect of planktonic foraminifera species-specific habitat on their oxygen isotopic content. *Geosci. Model Dev.* 11 (9), 3587–3603. Publisher: Copernicus GmbH.
- Rodríguez-Tovar, F.J., 2022. Ichnological analysis: a tool to characterize deep-marine processes and sediments. *Earth Sci. Rev.* 228, 104014.
- Rodríguez-Tovar, F.J., Hernández-Molina, F.J., 2018. Ichnological analysis of contourites: Past, present and future. *Earth Sci. Rev.* 182, 28–41.
- Röhl, U., Westerhold, T., Bralower, T.J., Zachos, J.C., 2007. On the duration of the Paleocene-Eocene thermal maximum (PETM). *Geochim. Geophys. Geosyst.* 8 (12).
- Royer, D.L., Berner, R.A., Beerling, D.J., 2001. Phanerozoic atmospheric CO₂ change: evaluating geochemical and paleobiological approaches. *Earth Sci. Rev.* 54 (4), 349–392.
- Ruddiman, W.F., Glover, L.K., 1972. Vertical Mixing of Ice-Rafted Volcanic Ash in North Atlantic Sediments. *GSA Bull.* 83 (9), 2817–2836.
- Ruddiman, W.F., Jones, G.A., Peng, T.H., Glover, L.K., Glass, B.P., Liebertz, P.J., 1980. Tests for size and shape dependency in deep-sea mixing. *Sed. Geol.* 25 (4), 257–276.
- Savrdra, C.E., Botjter, D.J., 1991. Oxygen-related biofacies in marine strata: an overview and update. *Geol. Soc. Lond., Spec. Publ.* 58 (1), 201–219.
- Schiffelbein, P., 1984. Effect of benthic mixing on the information content of deep-sea stratigraphical signals. *Nature* 311 (5987), 651–653.
- Schiffelbein, P., 1985. Extracting the benthic mixing impulse response function: a constrained deconvolution technique. *Mar. Geol.* 64 (3), 313–336.
- Schiffers, K., Teal, L.R., Travis, J.M.J., Solan, M., 2011. An Open Source Simulation Model for Soil and Sediment Bioturbation. *PLoS One* 6 (12), e28028.
- Seilacher, A., 1964. Sedimentological classification and nomenclature of trace fossils. *Sedimentology* 3 (3), 253–256.
- Shackleton, N.J., Lamb, H.H., Worssam, B.C., Hodgson, J.M., Lord, A.R., William, Shotton Frederick, Schove, D.J., Norman, Cooper Leslie Hugh, Francis, Mitchell George, Gilbert, West Richard, 1977. The oxygen isotope

- stratigraphic record of the Late Pleistocene. *Philos. Trans. R. Soc. Lond. B, Biol. Sci.* 280 (972), 169–182.
- Shull, D.H., 2001. Transition-matrix model of bioturbation and radionuclide diagenesis. *Limnol. Oceanogr.* 46 (4), 905–916.
- Siebert, C., Nögler, T.F., von Blanckenburg, F., Kramers, J.D., 2003. Molybdenum isotope records as a potential new proxy for paleoceanography. *Earth Planet. Sci. Lett.* 211 (1), 159–171.
- Smith, C.R., Rabouille, C., 2002. What controls the mixed-layer depth in deep-sea sediments? The importance of POC flux. *Limnol. Oceanogr.* 47 (2), 418–426.
- Smith, J.N., Boudreau, B.P., Noshkin, V., 1986. Plutonium and ²¹⁰Pb distributions in northeast Atlantic sediments: subsurface anomalies caused by non-local mixing. *Earth Planet. Sci. Lett.* 81 (1), 15–28.
- Soetaert, K., Herman, P.M.J., Middelburg, J.J., Heip, C., deStigter, H.S., vanWeering, T.C. E., Epping, E., Helder, W., 1996. Modeling Pb-210-derived mixing activity in ocean margin sediments: diffusive versus nonlocal mixing. *J. Mar. Res.* 54 (6), 1207–1227. WOS:A1996WC90100007.
- Solan, M., Ward, E.R., White, E.L., Hibberd, E.E., Cassidy, C., Schuster, J.M., Hale, R., Godbold, J.A., 2019. Worldwide measurements of bioturbation intensity, ventilation rate, and the mixing depth of marine sediments. *Sci. Data* 6 (1), 58.
- Soreghan, G.S., Cohen, A.S., 2013. Scientific drilling and the evolution of the earth system: climate, biota, biogeochemistry and extreme systems. *Sci. Drill.* 16, 63–72.
- Steffensen, J.P., Andersen, K.K., Bigler, M., Clausen, H.B., Dahl-Jensen, D., Fischer, H., Goto-Azuma, K., Hansson, M., Johnsen, S.J., Jouzel, J., et al., 2008. High-Resolution Greenland Ice Core Data Show Abrupt Climate Change Happens in Few Years. *Science* 321 (5889), 680–684.
- Tarhan, L.G., 2018. The early Paleozoic development of bioturbation—Evolutionary and geological consequences. *Earth Sci. Rev.* 178, 177–207.
- Tarhan, L.G., Droser, M.L., Planavsky, N.J., Johnston, D.T., 2015. Protracted development of bioturbation through the early Palaeozoic Era. *Nat. Geosci.* 8 (11), 865–869.
- Tarhan, L.G., Zhao, M., Planavsky, N.J., 2021. Bioturbation feedbacks on the phosphorus cycle. *Earth Planet. Sci. Lett.* 566, 116961.
- Teal, L., Bulling, M., Parker, E., Solan, M., 2010a. Global patterns of bioturbation intensity and mixed depth of marine soft sediments. *Aquat. Biol.* 2 (3), 207–218.
- Teal, L.R., Parker, E.R., Solan, M., 2010b. Sediment mixed layer as a proxy for benthic ecosystem process and function. *Mar. Ecol. Prog. Ser.* 414, 27–40.
- Thayer, C.W., 1979. Biological Bulldozers and the Evolution of Marine Benthic Communities. *Science* 203 (4379), 458–461.
- Thayer, C.W., 1983. Sediment-Mediated Biological Disturbance and the Evolution of Marine Benthos. In: Tevesz, M.J.S., McCall, P.L. (Eds.), *Biotic Interactions in Recent and Fossil Benthic Communities*, Topics in Geobiology. Springer, US, Boston, MA, pp. 479–625.
- Thomas, D.J., Zachos, J.C., Bralower, T.J., Thomas, E., Bohaty, S., 2002. Warming the fuel for the fire: Evidence for the thermal dissociation of methane hydrate during the Paleocene-Eocene thermal maximum. *Geology* 30 (12), 1067–1070.
- Thomas, E., 2003. Extinction and food at the seafloor: a high-resolution benthic foraminiferal record across the initial eocene thermal maximum, southern ocean site 690. *Spec. Pap. Geol. Soc. Am.* 319–332.
- Thomas, E., Zachos, J.C., 2000. Was the late Paleocene thermal maximum a unique event?. In: Schmitz, et al. (Eds.), *Early Paleogene Warm Climates and Biosphere Dynamics*, vol. 122. Taylor & Francis, pp. 169–170.
- Thomson, J., Cook, G.T., Anderson, R., MacKenzie, A.B., Harkness, D.D., McCave, I.N., 1995. Radiocarbon Age Offsets in Different-Sized Carbonate Components of Deep-Sea Sediments. *Radiocarbon* 37 (2), 91–101.
- Trauth, M.H., 1998. TURBO: a dynamic-probabilistic simulation to study the effects of bioturbation on paleoceanographic time series. *Comput. Geosci.* 24 (5), 433–441.
- Trauth, M.H., 2013. TURBO2: A MATLAB simulation to study the effects of bioturbation on paleoceanographic time series. *Comput. Geosci.* 61, 1–10.
- Trauth, M.H., Sarnthein, M., Arnold, M., 1997. Bioturbational mixing depth and carbon flux at the seafloor. *Paleoceanography* 12 (3), 517–526.
- van de Velde, S., Meysman, F.J.R., 2016. The Influence of Bioturbation on Iron and Sulphur Cycling in Marine Sediments: A Model Analysis. *Aquat. Geochem.* 22 (5), 469–504.
- van de Velde, S., Mills, B.J.W., Meysman, F.J.R., Lenton, T.M., Poulton, S.W., 2018. Early Palaeozoic ocean anoxia and global warming driven by the evolution of shallow burrowing. *Nat. Commun.* 9 (1), 2554.
- Weaver, P.P.E., Schultheiss, P.J., 1983. Vertical open burrows in deep-sea sediments 2 m in length. *Nature* 301 (5898), 329–331. Number: 5898 Publisher: Nature Publishing Group.
- Wefer, G., Berger, W.H., Bijma, J., Fischer, G., 1999. Clues to Ocean History: a Brief Overview of Proxies. In: Fischer, G., Wefer, G. (Eds.), *Use of Proxies in Paleoceanography: Examples from the South Atlantic*. Springer Berlin Heidelberg, Berlin, Heidelberg, pp. 1–68.
- Wetzel, A., 1984. Bioturbation in deep-sea fine-grained sediments: influence of sediment texture, turbidite frequency and rates of environmental change. *Geol. Soc. Lond., Spec. Publ.* 15 (1), 595–608.
- Wheatcroft, R.A., 1992. Experimental tests for particle size-dependent bioturbation in the deep ocean. *Limnol. Oceanogr.* 37 (1), 90–104.
- Wheatcroft, R.A., Jumars, P.A., Smith, C.R., Nowell, A.R.M., 1990. A mechanistic view of the particulate biodiffusion coefficient: step lengths, rest periods and transport directions. *J. Mar. Res.* 48, 177–207.
- Zonneveld, K.a.F., Versteegh, G.J.M., Kasten, S., Eglinton, T.I., Emeis, K.-C., Huguet, C., Koch, B.P., de Lange, G.J., de Leeuw, J.W., Middelburg, J.J., Mollenhauer, G., Prahl, F.G., Rethemeyer, J., Wakeham, S.G., 2010. Selective preservation of organic matter in marine environments; processes and impact on the sedimentary record. *Biogeosciences* 7 (2), 483–511.